Transportation Consortium of South-Central States

Solving Emerging Transportation Resiliency, Sustainability, and Economic Challenges through the Use of Innovative Materials and Construction Methods: From Research to Implementation

Developing Implementable Climatic Input Data and Moisture Boundary Conditions for Pavement Analysis and Design

Project No. 18POKS03

Lead University: Oklahoma State University

Final Report

August 2019

Disclaimer

The contents of this report reflect the views of the authors, who are responsible for the facts and the accuracy of the information presented herein. This document is disseminated in the interest of information exchange. The report is funded, partially or entirely, by a grant from the U.S. Department of Transportation's University Transportation Centers Program. However, the U.S. Government assumes no liability for the contents or use thereof.

Acknowledgements

The authors would like to acknowledge and thank the Project Review Committee (Dr. Omar Amer, Dr. Emad Kassem, and Dr. Arif Chowdhury) for their comments and suggestions. The authors also would like to thank Tran-SET for funding this important research study.

TECHNICAL DOCUMENTATION PAGE

1. Project No.	2. Government Accession No.	3. Recipient's Catalog No.
18POKS03		

4. Title and Subtitle	5. Report Date
Developing Implementable Climatic Input Data and Moisture Boundary Conditions for Pavement Analysis and Design	Aug. 2019
	6. Performing Organization Code
7. Author(s)	**8. Performing Organization Report No.**
PI: Rifat Bulut https://orcid.org/0000-0001-6047-1873 GRA: Amir Hossein Javid https://orcid.org/0000-0002-6783-9607	
9. Performing Organization Name and Address	**10. Work Unit No. (TRAIS)**
Transportation Consortium of South-Central States (Tran-SET) University Transportation Center for Region 6 3319 Patrick F. Taylor Hall, Louisiana State University, Baton Rouge, LA 70803	**11. Contract or Grant No.** 69A3551747106
12. Sponsoring Agency Name and Address	**13. Type of Report and Period Covered**
United States of America Department of Transportation Research and Innovative Technology Administration	Final Research Report Mar. 2018 – Mar. 2019
	14. Sponsoring Agency Code

15. Supplementary Notes

Report uploaded and accessible at Tran-SET's website (http://transet.lsu.edu/).

16. Abstract

The main objective of this study is to develop a practical and implementable numerical model for predicting the moisture (suction) regime within the pavement subgrade system. The research quality and uniformly-dispersed climate data over short distances from Oklahoma Mesonet and the Mitchell based moisture (suction) prediction methods establish the main background of the research study. The study involved numerical modeling and statistical analysis of climatic weather data. The proposed moisture variation model predicts the suction distribution throughout the soil subgrade by solving the diffusion equation and incorporates the measured suction from the Oklahoma Mesonet to estimate the diffusion coefficient. The research study resulted in a practical prediction model that could be used to determine the moisture boundary conditions within the pavement structure.

17. Key Words	18. Distribution Statement
Climate, Soil, EICM, TMI, Moisture, Suction	No restrictions. This document is available through the National Technical Information Service, Springfield, VA 22161.

19. Security Classif. (of this report)	20. Security Classif. (of this page)	21. No. of Pages	22. Price
Unclassified	Unclassified	50	

Form DOT F 1700.7 (8-72) **Reproduction of completed page authorized.**

SI* (MODERN METRIC) CONVERSION FACTORS

APPROXIMATE CONVERSIONS TO SI UNITS

Symbol	When You Know	Multiply By	To Find	Symbol
		LENGTH		
in	inches	25.4	millimeters	mm
ft	feet	0.305	meters	m
yd	yards	0.914	meters	m
mi	miles	1.61	kilometers	km
		AREA		
in^2	square inches	645.2	square millimeters	mm^2
ft^2	square feet	0.093	square meters	m^2
yd^2	square yard	0.836	square meters	m^2
ac	acres	0.405	hectares	ha
mi^2	square miles	2.59	square kilometers	km^2
		VOLUME		
fl oz	fluid ounces	29.57	milliliters	mL
gal	gallons	3.785	liters	L
ft^3	cubic feet	0.028	cubic meters	m^3
yd^3	cubic yards	0.765	cubic meters	m^3
		NOTE: volumes greater than 1000 L shall be shown in m^3		
		MASS		
oz	ounces	28.35	grams	g
lb	pounds	0.454	kilograms	kg
T	short tons (2000 lb)	0.907	megagrams (or "metric ton")	Mg (or "t")
		TEMPERATURE (exact degrees)		
^oF	Fahrenheit	5 (F-32)/9 or (F-32)/1.8	Celsius	^oC
		ILLUMINATION		
fc	foot-candles	10.76	lux	lx
fl	foot-Lamberts	3.426	$candela/m^2$	cd/m^2
		FORCE and PRESSURE or STRESS		
lbf	poundforce	4.45	newtons	N
lbf/in^2	poundforce per square inch	6.89	kilopascals	kPa

APPROXIMATE CONVERSIONS FROM SI UNITS

Symbol	When You Know	Multiply By	To Find	Symbol
		LENGTH		
mm	millimeters	0.039	inches	in
m	meters	3.28	feet	ft
m	meters	1.09	yards	yd
km	kilometers	0.621	miles	mi
		AREA		
mm^2	square millimeters	0.0016	square inches	in^2
m^2	square meters	10.764	square feet	ft^2
m^2	square meters	1.195	square yards	yd^2
ha	hectares	2.47	acres	ac
km^2	square kilometers	0.386	square miles	mi^2
		VOLUME		
mL	milliliters	0.034	fluid ounces	fl oz
L	liters	0.264	gallons	gal
m^3	cubic meters	35.314	cubic feet	ft^3
m^3	cubic meters	1.307	cubic yards	yd^3
		MASS		
g	grams	0.035	ounces	oz
kg	kilograms	2.202	pounds	lb
Mg (or "t")	megagrams (or "metric ton")	1.103	short tons (2000 lb)	T
		TEMPERATURE (exact degrees)		
^oC	Celsius	1.8C+32	Fahrenheit	^oF
		ILLUMINATION		
lx	lux	0.0929	foot-candles	fc
cd/m^2	$candela/m^2$	0.2919	foot-Lamberts	fl
		FORCE and PRESSURE or STRESS		
N	newtons	0.225	poundforce	lbf
kPa	kilopascals	0.145	poundforce per square inch	lbf/in^2

TABLE OF CONTENTS

TECHNICAL DOCUMENTATION PAGE ii
TABLE OF CONTENTS iv
LIST OF FIGURES vi
LIST OF TABLES viii
ACRONYMS, ABBREVIATIONS, AND SYMBOLS ix
EXECUTIVE SUMMARY xi
1. INTRODUCTION 1
2. OBJECTIVES 2
3. LITERATURE REVIEW 3
3.1. Enhanced Integrated Climatic Model (EICM) 3
3.2. Moisture Variation Prediction Models 4
3.2.1. Water Content-Based Methods 4
3.2.2. Suction-Based Methods 5
3.2.3. Seepage Analysis-Based Methods 5
3.3. Equilibrium Suction for Subgrade Soil 6
4. METHODOLOGY 8
4.1. Oklahoma Mesonet Climate Data 8
4.1.1. Oklahoma Mesonet Station Layout 9
4.1.2. Climate and Soil Moisture/Suction Data 10
4.1.3. Percent Sunshine from Solar Radiation 11
4.2. Thornthwaite Moisture Index 11
4.2.1. Thornthwaite (1948) Equation 12
4.2.2. Thornthwaite and Mather (50) Equation 13
4.2.3. Witczak et al. (57) Equation 13
4.3. Soil Suction Beneath Pavement 14
4.4. Seepage Analysis Based Models 15
4.4.1. Conservation of Mass 15
4.4.2. Flow Laws 16
4.4.3. PDE for One-dimensional Seepage 17

4.4.4. Boundary Conditions in Seepage 17
4.4.5. Soil-Water Characteristic Curve 18
4.4.6. Hydraulic Conductivity Estimation 18
4.4.7. Soil Atmosphere Interaction Modeling 19
4.5. Surface Suction Function 20
5. ANALYSIS AND FINDINGS 23
5.1. Proposed Prediction Model 23
5.1.1. Diffusion Coefficient 24
5.2. Seepage Analysis Based Model using Finite Element Method 25
5.2.1. Soil–atmosphere interaction for the Oklahoma Mesonet sites 25
5.3. Comparison of Results 27
5.3.1. ARD2 Station 27
5.3.2. DURA Station 30
5.3.3. HUGO Station 33
5.4. Correlation Between Environmental Parameters and Suction 37
5.4.1. Equilibrium Suction Model 37
5.3.2. Error Analysis 39
5.4. Guidelines for Analyzing Relevant Climate Data for Pavement Analysis 39
6. CONCLUSIONS 42
REFERENCES 43

LIST OF FIGURES

Figure 1. Distribution of Mesonet weather stations across Oklahoma (www.mesonet.org). 9

Figure 2. Campbell scientific 229-L sensor. 10

Figure 3. TMI contour map based on Thornthwaite and Mather *(65)* method. 13

Figure 4. TMI contour map based on Witczak et al. *(57)* method. 14

Figure 5. Monthly mean matric suction at 5 cm, 25 cm and 60 cm depths in Lane station, Atoka county, Oklahoma during 2017. 15

Figure 6. Suction distribution profile with respect to measured suction at 25 cm depth on 06/10/2017 at Ardmore, Carter county, Oklahoma. 24

Figure 7. The 1D SVFlux moisture migration model. 26

Figure 8. Climatic data collected at the ARD2 station in 2018, time series of air temperature. .. 28

Figure 9. Climatic data collected at the ARD2 station in 2018, time series of relative humidity. 28

Figure 10. Climatic data collected at the ARD2 station in 2018, time series of wind speed..... 29

Figure 11. Climatic data collected at the ARD2 station in 2018, time series of precipitation. 29

Figure 12. Climatic data collected at the ARD2 station in 2018, time series of net solar radiation. 30

Figure 13. Predicted soil suction profiles at 09/04/2018 - ARD2 station in 2018. 30

Figure 14. Climatic data collected at the DURA station in 2018, time series of air temperature. 31

Figure 15. Climatic data collected at the DURA station in 2018, time series of relative humidity. 31

Figure 16. Climatic data collected at the DURA station in 2018, time series of wind speed. 32

Figure 17. Climatic data collected at the DURA station in 2018, time series of precipitation..... 32

Figure 18. Climatic data collected at the DURA station in 2018, time series of net solar radiation. 33

Figure 19. Predicted soil suction profile at 09/18/2018 - DURA station in 2018. 33

Figure 20. Climatic data collected at the HUGO station in 2018, time series of air temperature. 34

Figure 21. Climatic data collected at the HUGO station in 2018, time series of relative humidity. 34

Figure 22. Climatic data collected at the HUGO station in 2018, time series of wind speed. 35

Figure 23. Climatic data collected at the HUGO station in 2018, time series of precipitation. ... 35

Figure 24. Climatic data collected at the HUGO station in 2018, time series of net solar radiation. 36

Figure 25. Predicted soil suction profile at 09/17/2018 - HUGO station in 2018. 36

Figure 26. Correlation between the equilibrium suction and Clay content (a), TMI (b), Relative humidity (c), and Relative humidity vs. TMI (d). 38

LIST OF TABLES

Table 1. Diffusion coefficient prediction from 15 Mesonet stations. 25

Table 2. Soil properties for three Mesonet stations. 25

ACRONYMS, ABBREVIATIONS, AND SYMBOLS

CMS	Climatic-Material-Structural
CRREL	Cold Regions Research and Engineering Laboratory
EICM	Enhanced Integrated Climatic Model
ID	Infiltration and Drainage
MEPDG	Mechanical-Empirical Pavement Design Guidelines
NCDC	National Climatic Data Center
NCHRP	National Cooperative Highway Research Program
OCS	Oklahoma Climatological Survey
SWCC	Soil Water Characteristics Curve
TMI	Thornthwaite Moisture Index
α	Diffusion coefficient
ΔT_{ref}	Reference temperature differential
a_s	Surface Short-Wave Absorptivity
D	Moisture Deficit
D_i	Day Length Correction Factor for The Month i
e_i	Unadjusted Potential Evapotranspiration
f_{cd}	Cloudiness Function
H_y	Annual Heat Index
MP	Soil Matric Suction
N_i	Number of Days in The Month i
P	Annual Precipitation
PE	Potential Evapotranspiration
Q_s	Net Short-Wave Radiation
R	Runoff
R_s	Measured or Predicted Solar Radiation
R_{so}	Predicted Clear-Sky Radiation
R^*	Extraterrestrial Radiation
S_c	Percent Sunshine

t	Time
t_i	Mean Monthly Temperature
u	Soil Suction
U_e	Equilibrium Suction Below the Moisture Active Zone Depth
U_m	Fourier Coefficients
U_o	Amplitude of Suction Variation
x	Coordinate
y	Depth of measured suction

EXECUTIVE SUMMARY

The current study mainly focused on improving our understanding of environmental interactions with pavement systems to better predict the changes in pavement material properties over time. The main objective of this study is to develop a practical and implementable numerical model for predicting the moisture (suction) regime within the pavement subgrade system. The research quality and uniformly-dispersed climate data over short distances from Oklahoma Mesonet and the Mitchell based moisture (suction) prediction method establish the main background of the research study.

The Oklahoma Mesonet data was utilized in developing the climate boundary conditions for the predictive model proposed in this study. Oklahoma has a unique and large cluster of Mesonet weather stations dispersed across the state. The Oklahoma Mesonet program started in 1991 as a statewide mesoscale environmental monitoring network with at least one station in each of Oklahoma's 77 counties. The Oklahoma Mesonet is a network of 121 automated weather monitoring stations designed to measure the weather and soil moisture conditions. A number of counties have more than one weather station. The primary focus of the Mesonet operations is to obtain research quality data in real time. The Oklahoma Mesonet follows a systematic, rigorous, and continuous monitoring protocol to verify the quality of all measurements.

The proposed moisture variation model predicts the suction distribution throughout the soil subgrade by solving the diffusion equation and incorporates the measured suction from the Oklahoma Mesonet to estimate the diffusion coefficient. The research study resulted in a practical prediction model that could be used to determine the moisture boundary conditions within the pavement structure. The proposed model was tested, and the results were compared with the predicted values from the well-established climatic models in the literature.

On the basis of the field data and numerical modeling, the study builds a relationship between equilibrium suction of subgrade soils, TMI, relative humidity and clay content. The matric suction under the unbound layer beneath the pavement can be estimated with environmental parameters and clay content. TMI and relative humidity are found to be controlling parameters in matric suction. The TMI, which effectively quantifies the environmental factors for a given region, can be obtained from contour maps developed in this study.

Thornthwaite Moisture Index (TMI) controls the moisture boundary conditions in the pavement profile. In this study, large cluster of raw climate and soil moisture data were obtained from Oklahoma Mesonet for assessment of the TMI from 1994 to 2017. Extensive computations have been carried out and TMI is calculated for 77 Mesonet weather stations representing 77 counties in the state. Thornthwaite Moisture Index (TMI) contour maps were created for Oklahoma using two different models.

1. INTRODUCTION

Environmental conditions have a significant effect on the pavement performance. Of all the environmental factors, temperature and moisture have direct effect on the pavement layer and subgrade properties. As a result, improving the understanding of environmental interactions with pavement systems can help predict the changes in pavement material properties over time. The current AASHTOWare Pavement ME software package utilizes the enhanced integrated climatic model (EICM) for applying the effects of climate on the pavement materials. The EICM was originally developed by integrating several earlier models in order to predict the flow of water and heat through layered pavement materials. The EICM plays a significant role in defining the material properties in the AASHTOWare Pavement ME computer program. The software uses historical climatic files that have been developed for each state in the US. However, these files are in most cases limited in number and region within each state, and therefore cannot represent the site-specific climate information. Furthermore, a number of states conducting research studies have found that there are significant discrepancies between the EICM predictions and measured values in the field. The differences are mainly attributed to insufficient climate data and deficiencies in the predictive models in the EICM. Therefore, there is a need to develop practical and implementable predictive models to study the moisture regime within the pavement subgrade in response to site specific climate data.

Oklahoma has a unique and large cluster of Mesonet weather stations dispersed across the state. The Oklahoma Mesonet program started in 1991 as a statewide mesoscale environmental monitoring network with at least one station in each of Oklahoma's 77 counties. The Oklahoma Mesonet is a network of 121 automated weather monitoring stations designed to measure the weather and soil moisture conditions. A number of counties have more than one weather station. The primary focus of the Mesonet operations is to obtain research quality data in real time. The Oklahoma Mesonet follows a systematic, rigorous, and continuous monitoring protocol to verify the quality of all measurements. Due to these features, the Oklahoma Mesonet data can be utilized in developing the climate boundary conditions for the predictive model proposed in this study.

This study mainly focused on improving our understanding of environmental interactions with pavement systems so that better predictions of the changes in pavement material properties over time can be made. The main objective of this study is to develop implementable, realistic climatic input data, and to develop a practical and implementable numerical model for predicting the moisture regime within the pavement subgrade system. The study aligns with the Tran-SET UTC's vision to use innovative techniques to overcome transportation challenges in Region-6.

2. OBJECTIVES

The main objective of this study is to develop a practical and implementable numerical model to evaluate the moisture regime within the pavement subgrade in response to site specific climate data. This study is also aimed at developing implementable, realistic climatic input data for establishing moisture boundary conditions above and below the subgrade soil within the moisture active zone.

The specific objectives of this study can be listed as follows:

1. Collect and evaluate research quality climate data from Oklahoma Mesonet;
2. Develop a practical and implementable moisture regime prediction model; and
3. Compare the new model using the well-established models in the literature.

3. LITERATURE REVIEW

Analysis of water flow through pavement subgrade system is an important part of the site-specific design of pavements. The performance of a pavement depends on many factors such as the structural adequacy, the properties of the materials used, traffic loading, climatic conditions and the construction methods *(1)*. Since unbound materials (subgrade soils and base course) are significant portions of the construction of pavements, much of the distress, particularly for flexible pavements, can be traced to problems in these materials. The performance specifications of pavements should be based on the short and long-term behavior of unbound materials in terms of the principals of unsaturated soil mechanics and seasonal variation of material properties in response to climate. The Enhanced Integrated Climatic Model (EICM), which is an integral component of the current AASHTO Pavement ME, plays an important role in defining the short and long-term pavement materials properties used in the design guide. The EICM involves analysis of water and heat flow through pavement layers in response to climatic, soil, and boundary conditions above and below the ground surface in pavement structures. The goal of the mechanistic design guide is to provide a quantitative and site-specific assessment of the pavement section needed to resist the traffic and environmental loading during the design lifetime *(2)*.

3.1. Enhanced Integrated Climatic Model (EICM)

Pavement performance is significantly affected by climatic interaction, specifically, where subgrade has poor drainage system and consists of fine grain soils. Currently, the Enhanced Integrated Climate Model (EICM) is utilized to predict the effect of climatic interaction with pavement materials. According to the Mechanical-Empirical Pavement Design Guide (MEPDG), results of EICM are used as an essential input for long term pavement design. The EICM has been developed over a long period of time and utilized a statistical model of climate databases, a hydraulic model for gravity drainage of water through soil, a surface heat transfer model, and a one-dimensional diffusion model for coupled temperature and water flow including soil freezing and frost heave *(3-6)*. The original form of the EICM was formed by Lytton et al. *(7)* and has been further updated by other researchers i.e., Larson and Dempsey *(8)*.

The Pavement ME software simulates temperature and moisture profiles in the pavement structure and subgrade over the design life of a pavement using the EICM. The EICM was further refined in the new Pavement ME within NCHRP Project 1-37A. The EICM is composed of four major components: The Precipitation (PRECIP) Model *(7)*, the Infiltration and Drainage (ID) Model *(5)*, the Climatic-Material-Structural (CMS) Model *(3)*, and the U.S. Army Cold Regions Research and Engineering Laboratory (CRREL) Model *(4)* for frost-heave-thaw settlement. The EICM was originally developed by integrating several previous models in order to predict the site-specific flow of water and heat through layered pavement materials. The major function of the EICM model in Pavement ME includes the prediction of the soil moisture content and soil water characteristics curve (SWCC) from the material grain size distribution and index properties, and the National Climatic Data Center (NCDC) database for sunshine, rainfall, wind speed, air temperature, and relative humidity. However, due to the multiple phenomena considered by this model and the complexity of the boundary conditions, the results from the EICM model are not well understood *(9)*.

The EICM has been tested independently by several states departments of transportation agencies in the U.S. including Arkansas *(10)*, Idaho *(11)*, Minnesota *(12)*, New Jersey *(13, 14)*, and Ohio

(15). Although all these states have been successful in matching their predictions of temperature with field data by some extend, all have observed poor performance in matching measured moisture (suction) distribution. This is mainly coming from complex characteristic of the model which was derived from (i) the empirical nature of several of the components of the model; (ii) the difference between the original developments of the component of models; (iii) the large number of needed inputs i.e., climatic variables, hydraulic properties of soils and pavement overlay, empirical "fitting" parameters that sometime is difficult to obtain for a location without site investigation or laboratory testing and (iv) only considering a one-dimensional moisture and temperature flow processes. By a careful evaluation of the EICM for different settings throughout the country, Zapata and Houston *(16)* observed an improvement in performance of the EICM analysis by specifying soil properties of site.

The EICM provides following outputs based on the climatic conditions at a road location (surface temperature and precipitation), drainage behavior of the aggregate base from initially saturated conditions, changes in pore water pressure and internal temperature distributions due to weather fluctuations, and the likelihood of freeze-thaw conditions. These outputs have been useful for design of drainage system and moisture barrier systems and have been correlated with the resilient moduli of the different pavement layers. Thus, validation of EICM outputs for pavement design is necessary and prevents over-design, resulting in high construction costs, or under-design, resulting in premature pavement failure.

3.2. Moisture Variation Prediction Models

The current methods of the prediction of moisture regime over time can be classified into three categories based on the state variables: (i) water content-based methods that use the soil water content as a state variable, (ii) suction-based methods that use the suction as a state variable, and (iii) seepage analysis.

3.2.1. Water Content-Based Methods

The soil movement due to environmental changes over time is related to soil suction changes. However, water content is more easily measured than matric suction and may be sufficient for predicting soil movement *(17)*.

Briaud et al. *(18)* proposed a water content method to estimate variations in water content, Δw, with depth and time. In their study, large water content databases were organized for several locations in Texas using the field investigations. The procedures for the method include: (1) Determine the depth Z_{max} of water content fluctuation and break the depth Z_{max} into an appropriate number of n layers, (2) Determine the change in water content, Δw as a function of depth within Z_{max}. Therefore, the range and the depth of water content variations can be estimated from a combination of experiences, databases, observations, and calculations. More details of this method are available in Briaud et al. *(18)*.

Overton et al. *(19)* conducted analysis of the migration of the wetting front using the commercial software VADOSE/W. VADOSE/W is a finite element program that can be used to model both saturated and unsaturated flows in response to the changes in atmospheric conditions while considering infiltration, precipitation, surface water runoff and ponding, plant transpiration and actual evaporation, and heat flow. The VADOSE/W model requires several inputs e.g., climate data, soil water characteristic curves, etc. The model is also required calibration by varying the

permeability functions of the clay. The results of the VADOSE/W modeling are VWC or Water content profiles for different sites conditions.

3.2.2. Suction-Based Methods

The moisture movement in unsaturated soils in terms of soil suction have been described by researchers in the field of geotechnical engineering *(20-26)*. Richards *(27)* proposed that the state of the soil water can be presented by the soil suction much more effectively than the water content for two reasons. Because soil suction is mainly controlled by the soil environment and not by the soil itself, and it characteristically does not exhibit discontinuous trends. The soil suction profile moves towards an equilibrium value at a particular depth which depends on climatic condition while water content is highly sensitive to the soil material variables (e.g., soil type, clay content, soil density, and soil structure). Moreover, the correlation between soil parameters (i.e. permeability or hydraulic conductivity, diffusivity, and shear strength) and water content is not significant unless other soil properties such as density and clay content are taken to account, however these parameters can be correlated with soil suction. More importantly, suction is considered as a stress state variable *(24)*.

Mitchell *(22)* suggested that the movement of water through unsaturated expansive soils can be adequately represented by diffusion equation in terms of soil suction expressed in pF units (Equation 11). Mitchell *(22)* solved the diffusion equation for the pavement structure moisture boundary conditions. The result was a suction profile beneath pavement based on monthly average surface suction. The diffusion coefficient in the model can be measured in the laboratory *(22)* or calculated from empirical equations *(28-30)*.

The Mitchell *(22)* method has been adopted both using the 3-D *(31)* (SUCH model) and the 1-D analysis *(28-30)*. However, the application of these studies to practical problems depends on the quantitative expression of the model parameters (i.e., the diffusion coefficient and the moisture active zone depth) and the initial and boundary conditions. In SUCH model, the initial soil suction value information is required for each nodal point. For this reason, it is a challenge to reliably measure field suctions especially in expansive soils.

Adem and Vanapalli *(32)* proposed a simple method using the soil-atmosphere model VADOSE/W to predict the variation of soil movement over time. The model has been developed based on the assumption that the soil is an isotropic and linear elastic material. Similar to Overton et al. *(19)* approach, VADOSE/W was used for simulating saturated and unsaturated flow in response to environmental changes. More details of this method are available in Adem and Vanapalli *(32)*.

3.2.3. Seepage Analysis-Based Methods

In most seepage problems involving soil-atmosphere interaction, infiltration and runoff must be considered. In the past empirical and semi-empirical functions have been proposed *(33, 34)*. However, more rigorous solutions, based on partial differential equations governing water flow and based on soil-atmosphere coupling equations were emerged *(35, 36)*.

Vu et al. *(37)* suggested that negative pore-water pressures (i.e., soil suctions) can be estimated through a saturated–unsaturated seepage analysis. The governing partial differential equation for saturated–unsaturated seepage is derived based on the following assumptions: (i) the air phase is continuous and remains at atmospheric pressure; (ii) soil is isotropic, nonlinear, and elastic. This

Seepage Analysis-based method mainly employs the Fredlund's approach in solving transient water flow problem *(38)*. Solving transient seepage problem required following soil properties namely, the coefficient of water volume change (or coefficient of water storage), the coefficient of permeability, and initial matric suction conditions. Both the coefficient of water storage and the saturated coefficient of permeability are predominant functions of matric suction. The coefficient of water storage is the slope of the soil water characteristic curve and can be obtained by differentiating the soil-water characteristic curve with respect to matric suction. Numerous equations have been proposed to simulate the soil-water characteristic curve *(39-41)*. The coefficient of permeability function can be indirectly computed or estimated from the soil-water characteristic curve and the saturated coefficient of permeability. There are several equations for the coefficient of permeability that have been proposed to represent the permeability function of an unsaturated soil *(39, 42, 43)*. Therefore, it is a challenge to reliably estimate of coefficient of water storage and permeability and field suctions especially in expansive soils.

Abed et al. *(44)* conducted the unsaturated ground water flow analysis to estimate the field suction variations. The PLAXFLOW finite element code *(45)* was used to simulate the unsaturated ground water flow and to determine the suction variation with time. The transient flow calculations for the infiltration and evaporation processes are very helpful. By applying transient boundary conditions, the variation of a suction profile with time can be simulated. Limitations of this approach are (i) the initial condition of suction, which was generated using the PAXFLOW code, and (ii) a relatively small suction increment Δs is required to insure numerical stability during stress integration.

3.3. Equilibrium Suction for Subgrade Soil

Previous studies showed that matric suction in the subgrade soil within the center area of the pavement reaches an equilibrium condition several years after construction *(46, 47)*. More importantly to predict pavement performance, an accurate estimate of equilibrium suction in the subgrade is critical for determining the volume change and long-term resilient modulus of subgrade soil. Current studies revealed that many factors affect the suction profile including precipitation, evapotranspiration, field capacity, etc. *(4, 49)*. These studies aimed at developing an improved prediction model of equilibrium suction, which would take into account a variety of influence factors.

Thornthwaite Moisture Index (TMI) was developed by Thornthwaite (*50)* and correlated with various annual moisture balance parameters. TMI was also correlated with the depth of moisture active zone and equilibrium suction *(51-53)*. Gay *(54)* developed a relationship between mean annual moisture depth and TMI. He used climatic data from 12 sites in Texas to find a correlation between TMI values and mean moisture depth. The Post Tensioning Institute (PTI) and the Australian standard AS2870 (2011) have also established a correlation between the TMI and subgrade equilibrium suction.

However, existing studies showed that suction beneath covered areas was dependent on both climatic factors and soil index properties *(48, 55, 56)*. Recently, Witczak, Zapata and Houston *(57)* proposed a statistical model to predict the subgrade equilibrium suction based on P_{200} and wPI parameters, where P_{200} is the percent of material passing no. 200 (0.075 mm) sieve and wPI is the product of P_{200} and plasticity index (PI). These correlation models were developed by using a limited number of data sets that are highly variable *(58)*. In this study, the accuracy of equilibrium

suction prediction model was improved by adopting a mechanistic-empirical approach which involved the suction profile and clay content as well as climatic factors.

4. METHODOLOGY

This research study collected and evaluated the data obtained from Oklahoma Mesonet from 1994 to 2017. This was an extremely large cluster of climate data to evaluate and analyze. The TMI and matric suctions are computed from the collected climatic data. The numerical modelling was utilized, and the Mitchell *(22)* model was used to predict and calculate equilibrium matric suctions from field suction measurements data.

The research quality data is available from Oklahoma Mesonet since the year 1994. The Oklahoma Mesonet system is preferred in this study mainly because the climate data is rigorously monitored and controlled, and more importantly the 121 weather stations across the state provide uniformly distributed data over short distances. These features enable the use of the Mesonet data and become an ideal platform in developing predictive models for moisture variations in subgrade soils.

4.1. Oklahoma Mesonet Climate Data

The Oklahoma Mesonet consists of 121 remote weather stations across Oklahoma which collect and report current weather and soil moisture conditions to a central computer facility every 15 minutes (Oklahoma Climatological Survey, climate.ok.gov). This is a unique network that covers short distances in the collection of the climate data in the U.S. *(59)*. The network was established jointly by Oklahoma State University and the University of Oklahoma in collaboration with the Climatological Survey and other public and private agencies in early 1990s. The Oklahoma Climatological Survey currently oversees Mesonet activities. Climatic variables are measured by a set of instruments located on or near a 10-meters (33 ft) tall tower, and below ground surface. On and above ground measurements include air temperature measurements at 1.5 m and 9 m above ground surface, wind speed at 2 m and 10 m, relative humidity at 1.5 m above the ground surface, solar radiation, barometric pressure, and rainfall. Soil temperature measurements at 5, 10, and 30 cm below the ground surface under bare and sod soil are recorded. Starting in 1996, the soil matric suctions have been measured by a large number of Campbell Scientific 229-L thermal conductivity sensors that were installed at depths of 5, 25, 60, and 75 cm below the ground surface. Figure 1 shows the distribution of the stations in Oklahoma. As of January 2007, the Oklahoma Mesonet includes soil moisture sensors at a depth of 5 cm at 103 sites, 25 cm at 101 sites, 60 cm at 76 sites, and 75 cm at 53 sites. The soil matric suction measurements are recorded every 30 minutes, 24 hours per day, and year-round. A detailed description of the thermal conductivity sensors can be found in *(60)*.

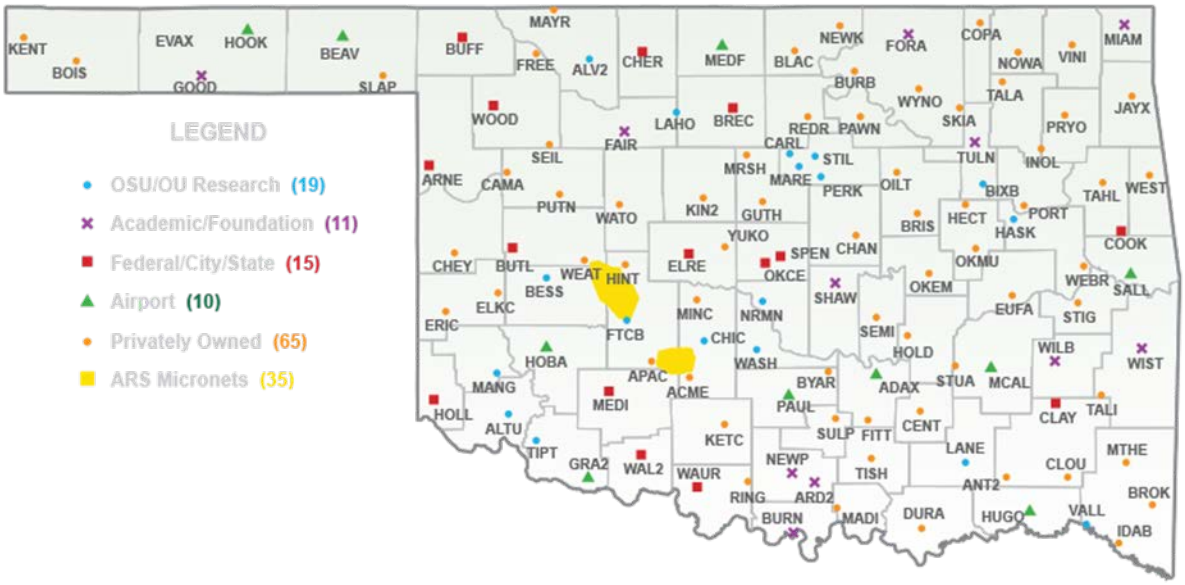

Figure 1. Distribution of Mesonet weather stations across Oklahoma (www.mesonet.org).

4.1.1. Oklahoma Mesonet Station Layout

Each Mesonet station send data (the observations) every 5 to 15 minutes to an operation and collection center located at the Oklahoma Climatological Survey (OCS) for verifying the quality of the data, data generation, storage, and dissemination. The mission of the OCS is to operate a world-class environmental monitoring network and to deliver high quality data to public and researchers *(59)*. One of the main objectives in establishing the Mesonet network was to ensure that a station site be as representative of as large an area as possible. Therefore, site locations for Mesonet stations fulfill a number of general requirements for meteorological and environmental purposes (mesonet.org): (1) rural sites should be selected to avoid human influences present in urban and suburban areas, (2) the physical characteristics of a site, including soil properties, should be representative of as large an area as possible, (3) a site should be as far away as possible from irrigated areas, lakes and forests to minimize their influence, (4) the land surface should be as flat as possible, (5) there should be a minimum of obstructions that impede wind flow at the site, and (6) sites should have a uniform low-cover vegetation. Bare soil should not be visible except over the bare soil temperature measurements

A Mesonet station occupies an area of about 10 m × 10 m (33 ft × 33 ft) and contains a datalogger, solar panel, radio transreceiver, lightning rod, and climate and environmental sensors located on or surrounding a 10 m high tower. The sensors measure more than 20 environmental and soil variables, the primary sensors are installed in all Mesonet sites and the secondary sensors are in about 100 sites. The stations are equipped with the Campbell Scientific dataloggers CR10X-TD and CR23X-TD for enhanced data storage and download. The 10 m high tower records the 5-minute average wind speed. The 5-minute average air temperature is measured by a sensor at a height of 1.5 meters above the ground. The total amount of precipitation is measured just above the ground in discrete tips of the bucket (approximately 0.01 inch per tip, or 0.254 millimeters). The average soil temperature during a 15-minute interval is measured at different depths below the ground where the surface is not vegetated.

4.1.2. Climate and Soil Moisture/Suction Data

Among 121 Mesonet stations shown in Figure 1, one station in each 77 counties of Oklahoma was selected to represent the climate of that county and to collect the relevant climate and soil moisture parameters for this study.

The hourly climatic data for the 77 selected stations has been obtained from the Oklahoma Mesonet. Each climatic file consists of pressure, temperature, dew point, relative humidity, wind direction, wind speed, maximum wind speed, precipitation, and solar radiation. Since the EICM input files require only five parameters, only those five parameters from the Mesonet files are selected. The temperature is the average air temperature at a height of 1.5 meters above the ground. The wind speed is the average wind speed measured at a height of 10 meters above the ground. The total amount of precipitation is measured just above the ground, and it is measured in discrete tips of the bucket. Relative humidity changes when either the air moisture or the air temperature changes. The relative humidity is measured at a height of 1.5 meters above the ground. Because of the sensor's inaccuracy, all the measurements above 100% are recorded as 100%. Measured solar radiation from the Mesonet is selected to calculate the percent sunshine. The solar radiation is measured by a sensor called Pyranometer. The pyranometer detect solar radiation which is reflected downward in the atmosphere.

Soil suction is a fundamental thermodynamic variable, and it is identical to the relative free energy of the soil moisture *(57)*. Recognizing the necessity of improving in-situ measurements of soil moisture, (suction), the Oklahoma Mesonet scientists designed the soil moisture measuring network to meet the needs from different disciplines. The soil moisture sensor installed at Oklahoma Mesonet sites is called the Campbell Scientific 229-L sensor (Figure 2) *(59)*. The sensor records the temperature change after a heat pulse has been introduced. Soil matric suction can be inferred by using the measured temperature difference. This sensor was chosen because of its small size, easy incorporation into the whole network, and absence of harmful radiation *(61)*.

Sensors were calibrated in laboratory before the installation, to remove the sensor-to-sensor variability. Next, the sensors were installed at multiple independent depths (5 cm, 25 cm, 60 cm, and 75 cm) to measure a temperature difference in the soil. The data are recorded every 30 minutes at each site, and the operation center, located at the Oklahoma Climatological Survey (OCS), remotely collects the data every 30 minutes as well *(59, 61)*. The soil matric suction can be inferred from the calibrated change in temperature of the soil over time after a heat pulse is introduced.

Figure 2. Campbell scientific 229-L sensor.

4.1.3. Percent Sunshine from Solar Radiation

The Mechanistic-Empirical Design Guide of New and Rehabilitated Pavement Structures (NCHRP 2004) *(62)* defined the percent sunshine as 0% for cloudy and 100% for clear sky. The percent sunshine is used to define the cloud cover in the sky. Therefore, the percent sunshine and percent cloud cover are direct opposite. Different methods have been developed to calculate the percent sunshine. Heitzman et al. *(63)* classified different percent sunshine values based on different categories of the sky coverage. Alternatively, a more universal approach has been developed as a part of an ASCE task force to standardize the evapotranspiration equation *(64)*.

$$f_{cd} = 1.35\frac{R_s}{R_{so}} - 0.35 \quad [1]$$

where:
The ratio R_s/R_{so} = the relative solar radiation (limited to $0.30 < R_s/R_{so} < 1.00$);
R_s = the measured or predicted solar radiation;
R_{so} = the predicted clear-sky radiation; and
f_{cd} = the cloudiness function (ranged between $0.05 < f_{cd} < 1.00$, which is dimensionless).

The National Cooperative Highway Research Program (NCHRP Report 2004) also suggests a very similar approach to calculate the percent sunshine.

$$Q_s = a_s R^*[A + B(\frac{S_c}{100})] \quad [2]$$

where:
Q_s = the net short-wave radiation;
a_s = the surface short-wave absorptivity;
A and B = Constants that account for diffuse scattering and adsorption, respectively;
S_c = the percent sunshine; and
R^* = the extraterrestrial radiation.

Both Equations 1 and 2 were evaluated in detail and the results were compared. The results have shown a small difference between the estimated percent sunshine obtained from these two methods.

This research study follows the NCHRP Equation 2 (as recommended by the MEPDG) to convert the measured solar radiation into an equivalent percent sunshine. Based on the NCHRP report recommendations, all the computed percent sunshine above 100% are recorded as 100% and all the values below 0% are recorded as 0%. Based on the obtained climate data from Oklahoma Mesonet, the measured solar radiation is zero during the night and reaches a maximum value around noon. By converting the measured solar radiation values into the equivalent percent sunshine, using the NCHRP approach, the computed results indicate that the values of percent sunshine are also zero during the night and reach the maximum around noon, and gradually decrease in the afternoon.

4.2. Thornthwaite Moisture Index

Thornthwaite Moisture Index (TMI) is an important climatic parameter widely used by geotechnical and pavement engineering community to predict the equilibrium soil suction beneath the moisture active zone, as well as the depth to constant suction. The total monthly precipitation, average monthly temperature, initial and maximum water storage values, the day length correction

factor, and the number of days for each month is required for calculating TMI. The precipitation and temperature values were obtained from the local weather stations. The maximum water storage which is a function of the soil type and the initial water storage depends on the climate and site conditions. The day length correction factor is a constant for a given month and location (latitude).

The standards for TMI climate classification are *(50)*:

$20 \leq TMI \leq 100$	Humid
$0 \leq TMI \leq 20$	Moist Sub-Humid
$-20 \leq TMI \leq 0$	Dry Sub-Humid
$-40 \leq TMI \leq -20$	Semi-Arid
$TMI \leq -40$	Arid

4.2.1. Thornthwaite (1948) Equation

Thornthwaite *(50)* adopted a relatively simple model for the calculation of the adjusted potential evapotranspiration as compared to some of the sophisticated (yet complex in terms of the parameters involved) models available in the literature. The adjusted potential evapotranspiration PET_i for the month, i, is calculated using the following equation:

$$PET_i = e_i(\frac{D_i N_i}{30}) \quad [3]$$

where:
D_i = Day length correction factor for the month i provided by McKeen and Johnson *(28)*;
N_i = Number of days in the month i; and
e_i = Unadjusted potential evapotranspiration (cm) for the month i calculated as:

$$e_i = 1.6(\frac{10t_i}{H_y})^a \quad [4]$$

where:
t_i = mean monthly temperature in °C; and
H_y = annual heat index that simply determined by summing the 12 monthly heat index values. The heat index for each month is determined as follows:

$$h_i = (0.2t_i)^{1.514} \quad [5]$$

and a is a coefficient given by:

$$a = 6.74 \times 10^{-7} H_y^3 - 7.17 \times 10^{-5} H_y^2 + 0.017921 H_y + 0.49239 \quad [6]$$

Thornthwaite *(50)* equation is given as:

$$TMI = \frac{(100R - 60D)}{PE} \quad [7]$$

where:
D = Moisture deficit;
R = Runoff; and
PE = Net potential evapotranspiration.

4.2.2. Thornthwaite and Mather (50) Equation

As mentioned previously, the original TMI method given by Thornthwaite *(50)* is computationally intensive and requires soil and moisture storage information that may not be readily available at many locations in Oklahoma or in the U.S. The simplified approach by Thornthwaite was later modified by Thornthwaite and Mather *(65)*. Figure 3 shows the contour maps developed using the modified Thornthwaite and Mather *(65)* method. The approach requires only precipitation and potential evapotranspiration at monthly intervals in evaluating the annual moisture index. The simplified equation is given as:

$$TMI = 100(\frac{P}{PE} - 1) \qquad [8]$$

where:
P = Annual precipitation; and
PE = Potential evapotranspiration.

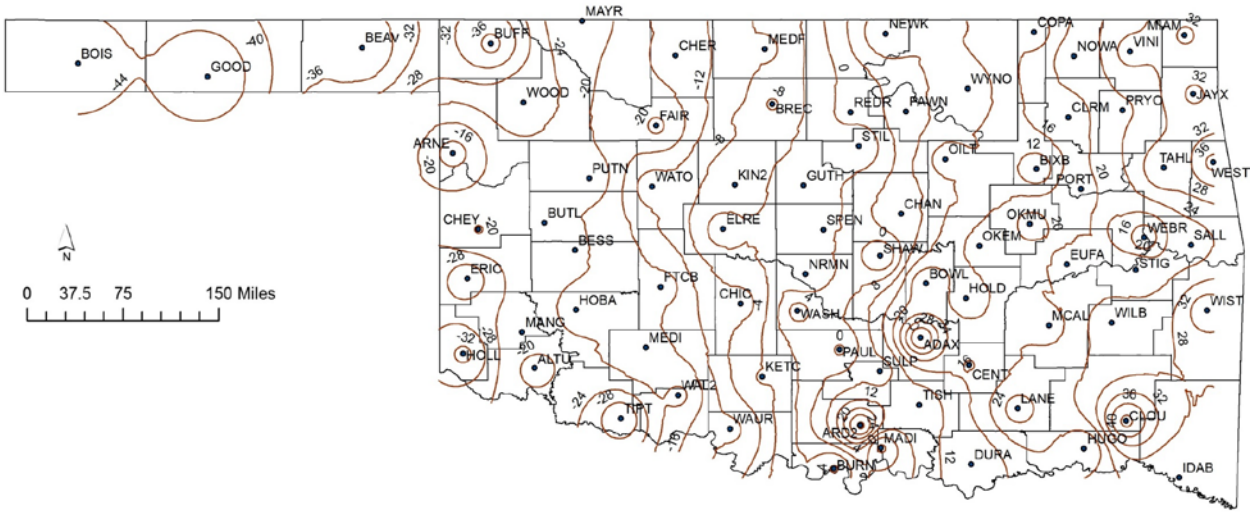

Figure 3. TMI contour map based on Thornthwaite and Mather *(65)* method.

4.2.3. Witczak et al. (57) Equation

In 2006, Thornthwaite *(50)* equation was modified as part of the NCHRP 1-40D research project for the development of the MEPDG Witczak et al. *(57)* and is given below:

$$TMI = 75\ (\frac{P}{PE} - 1) + 10 \qquad [9]$$

The TMI for Oklahoma is determined using the Witczak et al. *(57)* equation. Extensive computations have been carried out and TMI is calculated from 1994 to 2018 for the 77 Mesonet weather stations representing 77 counties in the state. The ArcGIS software is used to depict the TMI contour maps for Oklahoma. Contour maps consist of lines that connect points of equal values of TMI for a certain region. Figure 4 shows the contour maps developed using Witczak et al. *(57)* method.

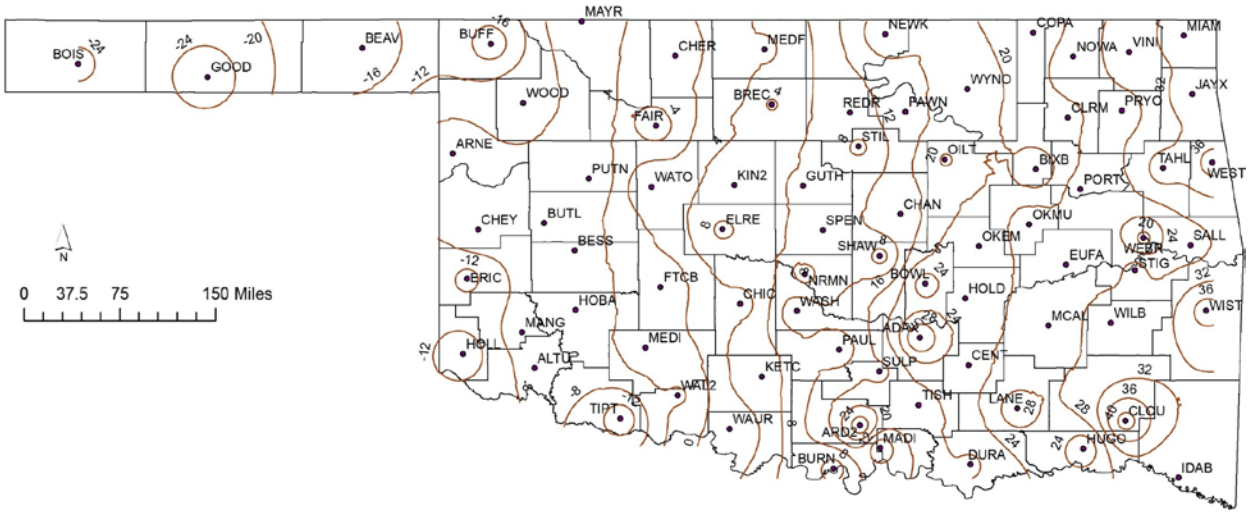

Figure 4. TMI contour map based on Witczak et al. *(57)* method.

4.3. Soil Suction Beneath Pavement

The Oklahoma Mesonet weather stations are equipped with CSI 229-L heat dissipation sensors at depths of 5 cm, 25 cm, 60 cm, and 75 cm. The sensors are capable of measuring the matric suctions indirectly through the heat dissipation capacity of the soil by measuring a temperature difference between two reference points. The correlation between temperature difference and matric suction of soil is given by the following equation *(59)*:

$$MP = -0.717e^{1.788\Delta T_{ref}} \quad [10]$$

where
MP = soil matric suction (kPa); and
ΔT_{ref} = reference temperature differential (°C).

Equation 10 was utilized to infer matric suction at various depths using temperature difference references obtained from Mesonet Stations. For instance, Figure 5 shows the monthly mean matric suctions for Lane station, Atoka county, Oklahoma during 2017.

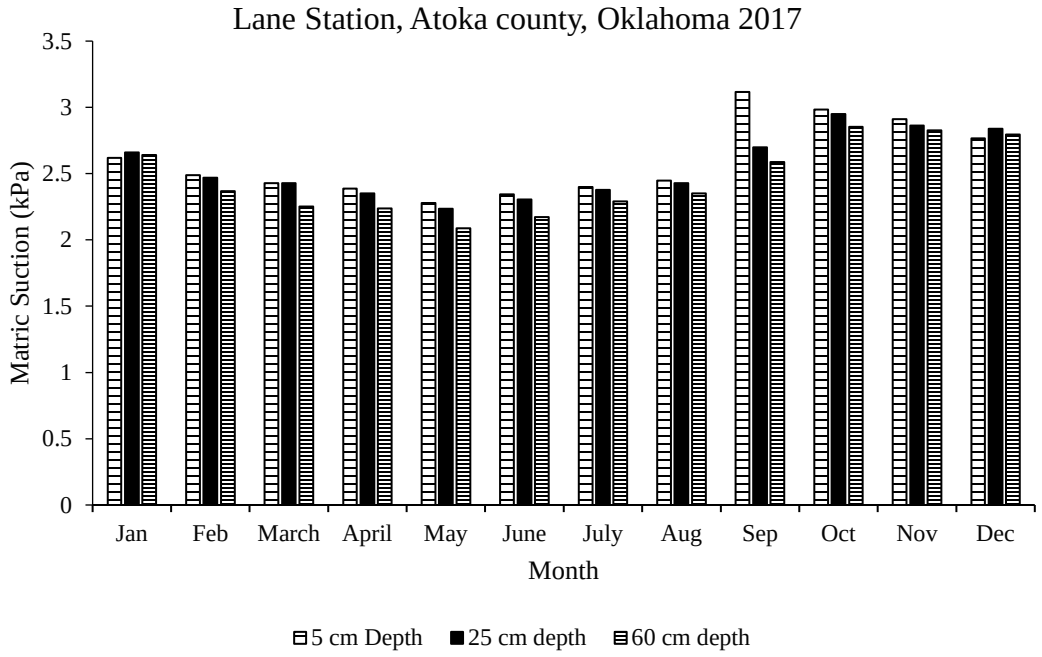

Figure 5. Monthly mean matric suction at 5 cm, 25 cm and 60 cm depths in Lane station, Atoka county, Oklahoma during 2017.

4.4. Seepage Analysis Based Models

Groundwater flow problems in geotechnical engineering generally involve the solution of a partial differential equation. Continuum mechanics principles and partial differential equations have been traditionally used for modeling seepage in saturated/unsaturated systems. The partial differential equations governing seepage may involve transient coupled soil-atmosphere processes with nonlinear and heterogeneous soil properties along with non-linear boundary conditions *(32, 66)*. Although it is considered as a more rational approach in terms of the principles of mechanics, constitutive laws and empirical equations as well as the input parameters involved, the seepage analysis-based model is a very cumbersome approach and requires significant amount of input parameters that are difficult to obtain.

4.4.1. Conservation of Mass

The fundamental law of conservation of mass of water is used to derive the governing equations for saturated/unsaturated seepage problems. A continuum mechanics framework is usually utilized to represent the fundamental conservation law. A differential equation of conservation of mass of water can be developed by considering a soil representative elemental volume and fluxes at the element faces (REV). The continuity equation can be derived by taking the flow rates in and out of the REV and equating the difference to the rate of change of mass in the REV with time. The Equation 11 is obtained by considering three-dimensional flow conditions *(66)*.

$$-\frac{\partial q_x^w}{\partial x}-\frac{\partial q_y^w}{\partial y}-\frac{\partial q_z^w}{\partial z}=\frac{1}{V_0}\frac{\partial M_w}{\eth t} \qquad [11]$$

where:

q_i^w = Total water flow rate in the i-direction across a unit area of the soil (kg/m^2-s);

V_0 = Referential volume, $V_0 = d_x d_y d_z$ (m^3);
M_w = Mass of water within the representative elemental volume (kg); and
t = Time (s).

Changes in Volume of Stored Water: The constitutive relationship for the amount of water stored in the soil pores is usually given in terms of volume of water. The change in volume of water stored in the soil pores can be expressed as function of coefficient of water storage, m_2^w as follow:

$$\frac{dV_w}{V_0} = m_2^w d(u_a - u_w) \qquad [12]$$

where:
$m_2^w = \frac{d(V_w/V_0)}{d(u_a - u_w)} = \frac{e}{1+e}\frac{dS}{d(u_a - u_w)}$;
V_w/V_0 = Volumetric water content;
e = Void ratio;
S = Degree of saturation; and
$(u_a - u_w)$ = Matric suction.

The above equation is based on the assumption that changes in the volume of pore-water stored in the soil are function of changes in soil suction and are independent of changes in total stress *(66)*.

4.4.2. Flow Laws

The flow rate of liquid water in saturated/unsaturated soils can be expressed by using a generalization of Darcy's law *(67)*. Where the driving mechanism is the total hydraulic head gradient. The hydraulic conductivity is considered to vary with matric suction. The generalized Darcy's law can be written as follows:

$$V_x^w = -k_x^w(\Psi)\frac{\partial h}{\partial x};\ V_y^w = -k_y^w(\Psi)\frac{\partial h}{\partial y};\ V_z^w = -k_z^w(\Psi)\frac{\partial h}{\partial z} \qquad [13]$$

where:
V_i^w = Liquid pore-water flow rate in the *i*-direction across a unit area of the soil due to hydraulic head gradients (m/s);
$k_i^w(\Psi)$ = Hydraulic conductivity in the *i*-direction (m/s);
h = Hydraulic head (m);
$h = \frac{u_w}{\gamma_w} + z$;
u_w = Pore-water pressure (kPa);
γ_w = Unit weight of water (kN/m^3); and
z = Elevation (m).

The hydraulic conductivity function, $k^w(\Psi)$ provides the relationship between the hydraulic conductivity and matric suction or volumetric water content.

The flow rate of water vapor due to gradients in vapor concentration can be described using a modified form of Fick's law *(68, 69)*.

$$V_x^v = -\frac{k^{vd}}{\gamma_w}\frac{\partial u_w}{\partial x};\ V_y^v = -\frac{k^{vd}}{\gamma_w}\frac{\partial u_w}{\partial y};\ V_z^v = -\frac{k^{vd}}{\gamma_w}\frac{\partial u_w}{\partial z} \qquad [14]$$

where:
k^{vd}= Pore-water vapor conductivity by vapor diffusion within the air phase;
$k^{vd} = \gamma_w \frac{W_v p_v}{\rho_w R(T+273.15)} \frac{D^{v*}}{\rho_w}$;
W_v = Molecular weight of water vapor, 18.016 (kg/kmol);
p_v = Partial pressure of water vapor (kPa);
R = Universal gas constant 8.314 (J/mol.k);
T = Temperature (°C);
D^{v*} = Vapor diffusivity through the soil (kPa);
$D^{v*} = \frac{(1-S)\, nD_v W_v}{RT}$ (kg.m/kN.s); and
D^v = Molecular diffusivity of vapor through soil (m^2/s).

The soil properties D^{v*} and D^vmust be directly measured or estimated by using the value of molecular diffusivity of vapor through air and combining that value with a tortuosity factor.

4.4.3. PDE for One-dimensional Seepage

In order to obtain the partial differential equation that governs the conservation of water mass (i.e., both liquid and vapor), the flow equations (Darcy and Fick's laws), and a water volume change constitutive equation must be combined with the continuity of water mass equation. Considering the reference volume V_0 is constant and water is incompressible, the following equation is obtained for one-dimensional transient saturated/unsaturated seepage *(66)*:

$$\frac{\partial}{\partial y}\left[(k_y^w + k^{vd})\frac{\partial h}{\partial y} - k^{vd}\right] = -\gamma_w m_2^w \frac{\partial h}{\partial t} \qquad [15]$$

where:
y = Coordinate in vertical direction, corresponding to elevation.

Three soil property functions can be identified in the transient seepage PDE; namely:

- Hydraulic conductivity function, k^w
- Vapor conductivity function, k^{vd}, and
- Soil-water characteristic curve, whose derivative with respect to matric suction represented by m_2^w.

These soil properties functions vary with soil suction.

4.4.4. Boundary Conditions in Seepage

The boundary conditions associated with the seepage analysis are as follows *(66)*:

- Natural boundary conditions: water flux.
- Essential boundary conditions: imposed water flux values or suctions.

Natural boundary conditions are appropriate choices for the representation of various situations, such as simple soil-atmosphere fluxes, the water uptake inside a well, and the groundwater flow taking place at the bottom of a domain. The natural boundary conditions associated with seepage PDEs do not make distinction between the type of flow (i.e., whether it is liquid or vapor flow).

Essential boundary conditions may be used to represent numerous situations, such as the head imposed to a surface by water reservoir or the head at the bottom of domain with relatively constant

water table. In steady state problems, essential boundary conditions are always required. Transient problem may or may not present an essential boundary condition.

4.4.5. Soil-Water Characteristic Curve

The soil-water characteristic curve is central to the application of unsaturated soil mechanics. Representation of the soil-water characteristic curve may be accomplished through either fitting existing data or estimating the curve from grain-size information *(39, 40, 42, 70-73)*.

Van Genuchten & Mualem Equation: The van Genuchten and Mualem *(71)* curve fitting model provides the soil-water characteristic curve given in Equation 16. It is similar in shape to the van Genuchten model but reduces the number of required curve fitting parameters by one through an assumed correlation between *n* and *m*.

$$W_w = W_{rm} + (W_s - W_{rm})[\frac{1}{[1+(a_m\psi)^{n_m}][1-\frac{1}{n_m}]}] \qquad [16]$$

where:
W_w = Volumetric water content at any soil suction;
W_{rm} = Residual volumetric water content;
W_s = Saturated volumetric water content;
a_m = A material parameter which is primarily a function of the air entry value of the soil (kPa);
n_m = A material parameter which is primarily a function of the rate of water extraction from the soil once the air entry value has been exceeded; and
ψ = Soil suction.

4.4.6. Hydraulic Conductivity Estimation

Equations available in the literature for predicting the coefficient of permeability use the soil-water characteristic curve data *(40, 73, 74)*. Several investigators including Brooks and Corey *(73)* and Mualem *(71)* have proposed closed-form equations to predict the coefficient of permeability of unsaturated soils based on Burdine's theory *(75)*. The Brooks and Corey *(73)* equation does not converge rapidly when used in numerical simulations of seepage in saturated-unsaturated soils. The Mualem *(71)* equation is in integral form and it is possible to derive a closed-form analytical equation provided a suitable equation is available for the soil-water characteristic curve.

The equation proposed for fitting the soil-water characteristic curve by van Genuchten *(40)* is flexible and a continuous function. The closed-form equation proposed for estimating the coefficient of permeability can be used for saturated-unsaturated seepage modeling.

$$K(\psi) = K_s[\frac{(1-(a\psi)^{nm}[1+(a\psi)^n]^{-m})^2}{[1-(a\psi)n]^{m/2}}] \qquad [17]$$

where:
K = Hydraulic conductivity or permeability of the water phase;
K_s = Saturated hydraulic conductivity of the water phase determined by the van Genuchten;
a = van Genuchten soil-water characteristic curve fitting parameter;
n = van Genuchten soil-water characteristic curve fitting parameter;
m = van Genuchten soil-water characteristic curve fitting parameter; and
ψ = Soil suction.

4.4.7. Soil Atmosphere Interaction Modeling

The water falling on the ground surface either infiltrates the soil at the same location, flows to somewhere else as runoff, or it is rises to the sky through the process called "Actual Evaporation". The ground surface moisture and thermal flux equations can be written as follows *(76)*.

$$P = AE + NP + R_{off} \quad [18]$$

$$Q_n = Q_h + Q_l + Q_g \quad [19]$$

where:
P = Precipitation (m/day);
AE = Actual evaporation from ground surface (m/day);
NP = Net percolation or infiltration (m/day);
R_{off} = Runoff (m/day);
Q_n = Net radiation (kJ/m^2) or converted into (m/day);
Q_h = Sensible heat transferring from ground surface to air (kJ/m^2) or converted into (m/day);
Q_l = Latent heat associated with the water phase change including evaporation or freezing (kJ/m^2) or converted into (m/day); and
Q_h = Ground heat flux (kJ/m^2) or converted into (m/day).

Precipitation information can be obtained from weather station records and is usually provided on a daily basis. The mechanics of net infiltration, NP, can be described by Darcy's law. Net radiation, Q_n, can also be obtained from weather station records or it can be approximated from solar radiation using the ASCE Standardized Reference Evapotranspiration Equation. The latent heat, Q_l, can be estimated using an actual evaporation, *AE*, or formation of ice near the ground surface during freezing. The sensible heat component, Q_h, reflected from the ground surface to the air is described as follows *(76-78)*:

$$Q_h = C_f \eta f(u)(T_s - T_a) \quad [20]$$

where:
Q_h = Sensible heat (m/day);
C_f = Conversion factor (i.e., $1kPa = 0.0075\ mHg$);
η = Psychometric constant $0.06733 \frac{kPa}{^\circ C} at\ 20^\circ C$;
$f(u)$ = Function depending on wind speed $f(u) = 0.35(1 + 0.146W_w)$; and
W_w = Wind speed (km/hr).

Actual Evaporation, *AE*, is difficult to measure directly but can be estimated from fundamental thermodynamics principles. Equations 18 and 19 are fundamental to describing the coupling of moisture and heat flow processes. Actual evaporation, *AE*, depends on the water content and temperature of soil at ground surface as well as the relative humidity in the air above ground surface. In addition, the rate of evaporation also depends on the air temperature. The air temperature and soil temperature at the ground surface are generally not of the same but are inter-related by the net radiation, Q_n, latent heat, Q_l, and sensible heat, Q_h. The available surface water controlled by total precipitation, actual evaporation, and runoff. These variables play important role in partitioning the convective heat flux into sensible heat and latent heat *(79)*.

Evaporation: The effects of evaporation on a soil near the ground surface depend on the suction gradient between the soil surface and the atmosphere. Potential evaporation, PE, is the amount of evaporation that would occur for the saturated soil. The potential evaporation at a material-atmosphere boundary can be calculated using the following formulation *(77)*:

$$PE = \frac{\Gamma Q_n + \eta E_a}{\Gamma + \eta} \quad [21]$$

where:
PE = Potential evaporation (m/day);
E_a = Flux associated with "mixing"; $f(u)C_f u_{c0}^{air}(1 - h_r)$ (m/day);
$f(u) = 0.35(1 + 0.146W_w)$;
W_w = Wind speed (km/hr);
C_f = Conversion factor (i.e., $1kPa = 0.0075\ mHg$);
h_r = Relative humidity in the air above the ground (i.e., $h_r = u_v^{air}/u_{v0}^{air}$);
u_v^{air} = Water vapor pressure in the air above ground surface (kPa);
u_{v0}^{air} = Saturated vapor pressure at the mean air temperature (kPa);
Γ = Slope of saturation vapor pressure vs. temperature curve ($kPa/$℃);
Q_n = Net radiation at the water surface (*m/day)*; and
η = Psychrometric constant, 0.06733 ($kPa/$℃).

The u_v^{air}, u_{v0}^{air} and Γ can be calculated from temperature as proposed by Lowe (*80)*.

$$u^{soil}{}_{vsat} = a_0 + a_1T_s + a_2T_s^2 + a_3T_s^3 + a_4T_s^4 + a_5T_s^5 + a_6T_s^6 \quad [22]$$

$$u^{air}{}_{vsat} = a_0 + a_1T_s + a_2T_s^2 + a_3T_s^3 + a_4T_s^4 + a_5T_s^5 + a_6T_s^6 \quad [23]$$

$$\Gamma = a_0 + 2a_2T_s + 3a_3T_s^2 + 4a_4T_s^3 + 5a_5T_s^4 + 6a_6T_s^5 \quad [24]$$

where:
T_s = Temperature at the material surface (℃);
T_a = Atmosphere air temperature (℃);
a_0 = 0.6183580754;
a_1 = 0.041142732;
a_2 = 0.0017217473;
a_3 = 0.000074108;
a_4 = 0.0000003985; and
a_5 = 0.0000000022.

The net radiation can be calculated using ASCE Standardized Reference Evapotranspiration Equation *(81)*. The detailed procedure to calculate the net radiation is discussed in ASCE Standardized Reference Evapotranspiration Equation which depends on the surface cover and quality of the data collected from weather station.

4.5. Surface Suction Function

The suction distribution throughout the soil subgrade can be predicted using the diffusion equation proposed by Mitchell *(22)*. According to Mitchell, suction change due to the effect of climate, drainage and site cover is a periodic function of time and can be determined by solving the diffusion equation for these boundary conditions.

$$\frac{\partial u}{\partial t} = \alpha \frac{\partial^2 u}{\partial x^2} \quad [25]$$

Boundary conditions:

$$u(o,t) = u_o \cos(wt)$$

$$u(x,t) \to 0 \; as \; x \; \to \infty$$

where:
u = Soil suction expressed as a pF;
α = Diffusion coefficient (cm^2/s);
t = Time (s); and
x = Coordinate.

The solution to the diffusion equation that solved by linear homogeneous equation of the fourth order is:

$$u(x,t) = U_o e^{-\sqrt{(\frac{w}{2\alpha}}x)} \cos(wt - \sqrt{(\frac{w}{2\alpha}}x) \quad [26]$$

If the soil surface subjected to a periodic suction change of frequency n, $u(o,t)$ can be written as:

$$u(o,t) = U_e + U_o \cos\ (2\pi nt) \quad [27]$$

Then the suction at any depth y can be written as:

$$u(y,t) = \ U_e + U_o e^{-\sqrt{(\frac{n\pi}{\alpha}}y} \cos(2\pi nt - \sqrt{(\frac{n\pi}{\alpha}}y) \quad [28]$$

where:
U_e = Equilibrium suction below the moisture active zone depth [pF (kPa)]; and
U_o = Amplitude of suction variation.

The equation is a function of the coefficient of diffusion; α and as depth increases the suction decreases exponentially.

Effect of climate variation can be expressed by imposing an arbitrary state of suction. The arbitrary state of suction as a function of time $u(o,t)$ and for any periodic function of period $2p = \frac{1}{n}$ can be written as a Fourier series. Thus, the total effect of $u(o,t)$ corresponds to sum of all the effect at each partial wave.

$$u(o,t) = \ \frac{U_o}{2} + U_1 \cos(n2\pi t) + U_2 \cos(2n2\pi t) + \cdots etc. \quad [29]$$

$$u(y,t) = \ \frac{U_o}{2} + U_1 \, \mathrm{e}^{-y\sqrt{(n\pi/\alpha)}} \cos(n2\pi t - y\sqrt{(n\pi/\alpha)}) +$$

$$U_2 \, \mathrm{e}^{-y\sqrt{(2n\pi/\alpha)}} \cos(2n2\pi t - y\sqrt{(2n\pi/\alpha)}) + \cdots etc. \quad [30]$$

where:
y = Depth of measured suction; and
U_0, U_1, U_2 …. etc.. = Fourier Coefficients which can determined from Equation 31.

$$U_m = \frac{2}{P}\int_0^p u(o,t) \cos(\frac{2m\pi t}{p})\, dt, \; m = 0, 1, 2 \ldots \quad [31]$$

Then for a period of 12 month, the Fourier coefficients can be written as

$$U_m = \frac{2}{12}\left[\int_0^1 S_1 \cos\frac{m\pi t}{6}\,dt + \int_1^2 S_2 \cos\frac{m\pi t}{6}\,dt + \cdots + \int_{11}^{12} S_{12} \cos\frac{m\pi t}{6}\,dt\right] \quad [32]$$

where:
$S_1, S_2, \ldots, S_{12}$ = Monthly average of the surface suction.

Equation 30 implies that the amplitude of suction at any depth decreases exponentially as a function of the coefficient of diffusion α,and that the suction at the depth *y* lags behind the suction at the surface $y = 0$ by a time equal to:

$$t = \frac{y}{2}\sqrt{\frac{1}{\alpha\pi n}} \quad [33]$$

where:
t = Time lag (s);
α = Diffusion coefficient (cm^2/s); and
y = Depth (cm).

5. ANALYSIS AND FINDINGS

This research study resulted in some practical guidelines that could be used to determine the moisture boundary conditions within the pavement structure. These boundary conditions can involve the maximum and minimum variations of the surface moisture conditions, and their variations with depth within the moisture active zone. The proposed moisture variation model was tested, and the results compared with the predicted values from a well-established climatic model in the literature.

5.1. Proposed Prediction Model

There are several moisture regime prediction models available in the literature. All these models (including EICM) are complicated and require substantial amount of input data and information. Mitchell *(22)* proposed a model that includes the pavement structure moisture boundary conditions.

In this study, the Mitchell *(22)* model is modified by incorporating the climate data collected on a regular basis from Oklahoma Mesonet weather stations. The Oklahoma Mesonet climate data are essential components of this study for the improvement of the model. The new model is a practical and implementable tool for pavement engineers in predicting site specific moisture variations underneath the pavement within the moisture active zone in response to wetting and drying weather cycles.

The suction change in soil due to the effects of climate, drainage and site cover is a periodic function of time. By solving the diffusion equation for these boundary conditions, the suction at any time at any depth in the soil profile can be determined. The results of the Mitchell model have shown moderate to good correlation with the field measurements of soil suction from Oklahoma Mesonet. However, the application of the Mitchell model to practical problems depends on the quantitative expression of the model parameters (i.e., the diffusion coefficient).

It is intended in this study that the Mitchell *(22)* is modified and improved by using surface suction functions as described in previous chapters and incorporating the climate data collected on a regular basis at weather stations. MATLAB was used to develop and predict the suction profile beneath pavement based on monthly average surface suction and measured suction surface for a day. The study utilized the climate data from nearest Oklahoma Mesonet to construct the suction profile. For instance, Figure 6 shows the suction distribution profile constructed by fitted measured suction for Ardmore, Carter County, Oklahoma. The modified Mitchell model successfully used the measured suction from the field and computed the diffusion coefficient.

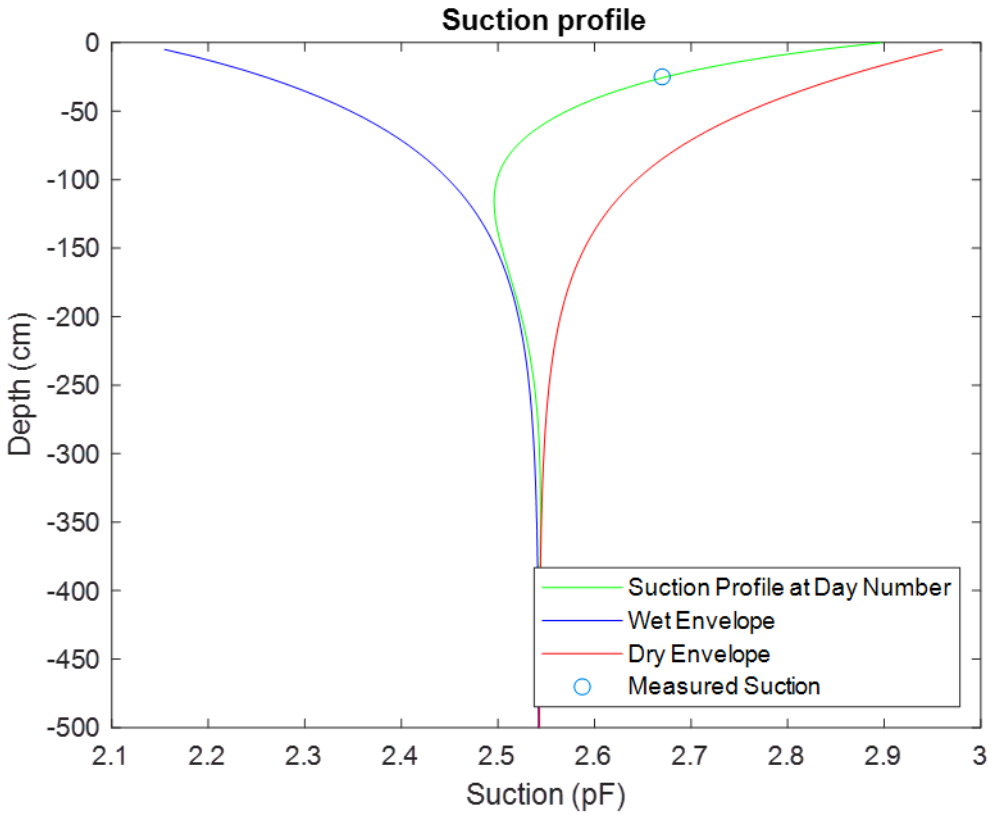

Figure 6. Suction distribution profile with respect to measured suction at 25 cm depth on 06/10/2017 at Ardmore, Carter county, Oklahoma.

5.1.1. Diffusion Coefficient

The magnitude and rate of transient moisture flow in an unsaturated soil in response to suction changes is controlled by the unsaturated moisture diffusion coefficient, which is a fundamental soil parameter in Mitchell's model. An attempt has been made to back calculate the diffusion coefficient by using a function that represents the suction change at the surface. The amplitude of the suction change decreased as the depth increased as given in Equation 16. As it was mentioned, amplitude also increases with increasing diffusion coefficient. Therefore, amplitude is a function of the diffusion coefficient of the soil. A successful approach was to plot the suction data versus depth with respect to time. The field data obtained near the surface were plotted and compared to calculated values from Equation 16 at various values of diffusion coefficient at similar depths. The value of the diffusion coefficient was selected by computing and fitting values from Equation 16 with respect to field data obtained near the surface. Table 1 shows the predicted diffusion coefficients for 15 Mesonet stations.

Table 1. Diffusion coefficient prediction from 15 Mesonet stations.

Station ID	City	County	Depth [cm (ft)]	Diffusion coefficient (cm^2/s)	Equilibrium suction [kPa (pF)]
ARD2	Ardmore	Carter	25 (0.8)	3.00E-05	33 (2.5)
ARNE	Arnett	Ellis	25 (0.8)	8.00E-04	43 (2.6)
BURN	Burneyville	Love	25 (0.8)	7.72E-04	26 (2.4)
CENT	Centrahoma	Coal	25 (0.8)	1.46E-05	15 (2.2)
CLOU	Cloudy	Pushmataha	25 (0.8)	3.84E-04	21 (2.3)
DURA	Durant	Bryan	25 (0.8)	4.23E-04	26 (2.4)
GOOD	Goodwell	Texas	25 (0.8)	8.53E-04	78 (2.9)
HUGO	Hugo	Choctaw	25 (0.8)	1.04E-04	22 (2.3)
JAYX	Tishomingo	Johnston	25 (0.8)	1.42E-04	17 (2.2)
LANE	Lane	Atoka	25 (0.8)	4.10E-04	35 (2.5)
MAYR	May Ranch	Woods	25 (0.8)	3.60E-04	56 (2.8)
SALL	Sallisaw	Sequoyah	25 (0.8)	7.74E-04	12 (2.1)
TIPT	Grandfield	Tillman	25 (0.8)	5.68E-04	21 (2.3)
VINI	Centralia	Craig	25 (0.8)	8.32E-04	22 (2.3)
WIST	Wister	LeFlore	25 (0.8)	7.43E-04	32 (2.5)

5.2. Seepage Analysis Based Model using Finite Element Method

This study used the SVFlux software package, *(82)*, to compare the results with the one-dimensional soil–atmosphere model, developed in this study, based on the measured climate data at three Oklahoma Mesonet sites. SVFlux makes use of a general finite element solver to solve the Richards equation for both saturated and unsaturated flow. The finite element solver makes use of automatic mesh generation and automatic mesh refinement techniques in solving flow problems.

5.2.1. Soil–atmosphere interaction for the Oklahoma Mesonet sites

The 1D SVFlux moisture migration model consists of a single layer soil with 5m thickness. The soil properties were collected from subsurface investigations that were performed by Scott et al. (*83)* to estimate the soil properties, including the saturated hydraulic conductivity k_s; percentages of sand, silt and clay; and the parameters defining the SWCCs. Table 2 shows the soil properties for three Mesonet sites in Oklahoma. The SWCCs describe the variation in soil moisture content with respect to changes in soil suction. In this study, the van Genuchten and Mualem SWCC (1975) method was adopted as described in the previous chapter. The SWCCs for this study obtained using the fitting parameters provided by Scott et al. *(83)*. The 1D soil–atmosphere interaction model created using SVFlux for the Oklahoma Mesonet sites is depicted in Figure 7.

Table 2. Soil properties for three Mesonet stations.

Station ID	Soil texture class	θ_s	θ_r	k_s (m/hr)	α (kPa^{-1})	n
ARD2	Clay loom	0.427	0.068	0.1188	0.078	1.252
DURA	Clay loom	0.402	0.064	0.161	0.12	1.262
HUGO	Clay	0.432	0.067	0.0844	0.08	1.354

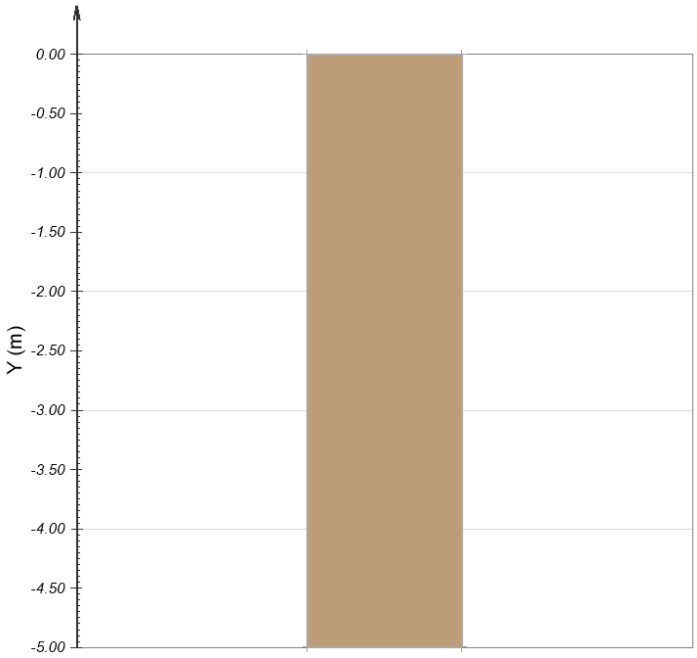

Figure 7. The 1D SVFlux moisture migration model.

Boundary Conditions: Hourly climatic data derived from Mesonet measurements were applied at the soil surface as a climatic boundary condition. Runoff was applied on the soil surface with the pounding height set to zero. By using the known station latitudes, longitudes and elevations, the methodology given by ASCE Standardized Reference Evapotranspiration Equation was applied to convert the incoming solar radiation measurements provided by the Mesonet data to net radiation, which is a parameter needed in the SVFlux Climate Manager.

Actual Evaporation: In 1994, Wilson proposed a modification to a well-known Penman *(77)* equation for the calculation of Potential Evaporation, *PE*. The modified equation has become known as the Wilson-Penman equation *(84)*. The Wilson-Penman equation takes into account the difference between the soil surface and air. This study adopted the Wilson-Penman *(84)* SVFlux model which has following assumptions:

- Moisture and vapor flow occur through the soil.
- The soil temperature in the entire domain is constant. In other words, the ground thermal flux is neglected.
- The soil temperature at the surface can be different from the air temperature. The heat exchanged between air and soil surface follows the convection law as given in Equation 20.
- Actual Evaporation is calculated using Wilson-Penman *(84)* equation. The Wilson-Penman (1994) equation for actual evaporation, AE, is written as follows:

$$AE = \frac{\Gamma Q_n + \eta E_a}{\Gamma + \eta / h_s} \quad [34]$$

where:
AE = Actual evaporation (m/day);
E_a = Flux associated with "mixing"; $f(u) C_f u_{c0}^{air} (1 - h_r)$ (m/day);

$f(u) = 0.35(1 + 0.146W_w)$;
W_w = Wind speed (km/hr);
C_f = Conversion factor (i.e., $1kPa = 0.0075\ mHg$);
h_r = Relative humidity in the air above the ground (i.e., $h_r = u_v^{air}/u_{v0}^{air}$);
h_s = Relative humidity at the soil surface (i.e., $h_s = u_v^{soil}/u_{v0}^{soil}$);
u_v^{air} = Water vapor pressure in the air above ground surface (kPa);
u_{v0}^{air} = Saturated vapor pressure at the mean air temperature (kPa);
u_v^{soil} = Vapor pressure in the soil at ground surface (kPa);
u_{v0}^{soil} = Saturated vapor pressure in the soil at ground surface (kPa);
Γ = Slope of saturation vapor pressure vs. temperature curve ($kPa/$°C);
Q_n = Net radiation at the water surface (*m/day)*; and
η = Psychrometric constant, 0.06733 ($kPa/$°C).

The parameter, Γ, is obtained from Equation 33.

$$\Gamma = 0.041142732 + 2 \times 0.0017217473T_s^1 + 3 \times 0.0000174108T_s^2 + 4 \times 0.0000003985T_s^3 + 5 \times 0.0000000022T_s^4 \quad [35]$$

5.3. Comparison of Results

In this section, soil suction profiles predicted by the Seepage Analysis Based Model are compared with the profiles predicted using the model developed in this study for three Oklahoma Mesonet sites for the year 2018.

5.3.1. ARD2 Station

The climatic data acquired from ARD2 station over a period of 8640 h (365 d) in 2018 are shown in Figures 8 to 12. The initial soil suction profile was assigned using equilibrium suction values estimated by the proposed model. The comparison of results between the proposed model and Finite Element (FE) Seepage simulation are presented in Figure 13. Overall, the proposed model and FE Seepage simulated soil suction values for ARD2 station over the time period of interest showed more variations near the surface. The FE Seepage simulated soil suction profile revealed drier soil near the surface for the time of the analysis (09/04/2018) while the proposed model predicted a suction profile in agreement with the measured suction on 09/04/2018 as shown in Figure 13.

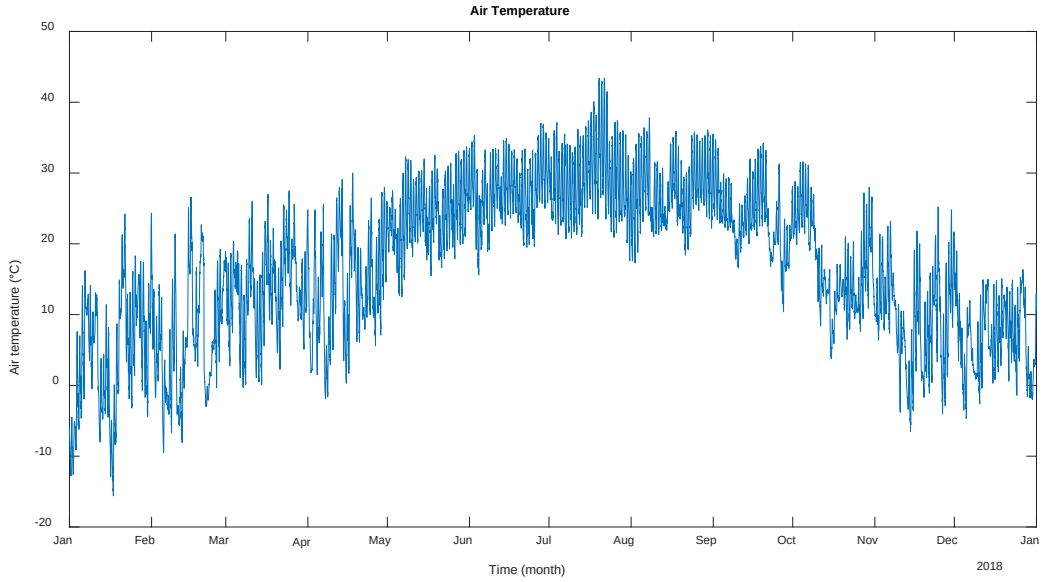

Figure 8. Climatic data collected at the ARD2 station in 2018, time series of air temperature.

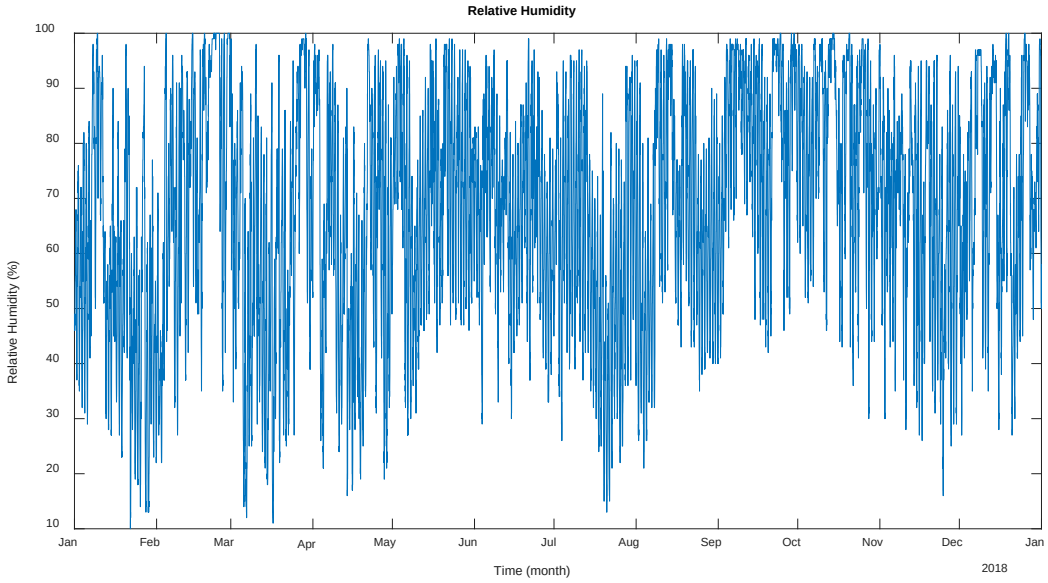

Figure 9. Climatic data collected at the ARD2 station in 2018, time series of relative humidity.

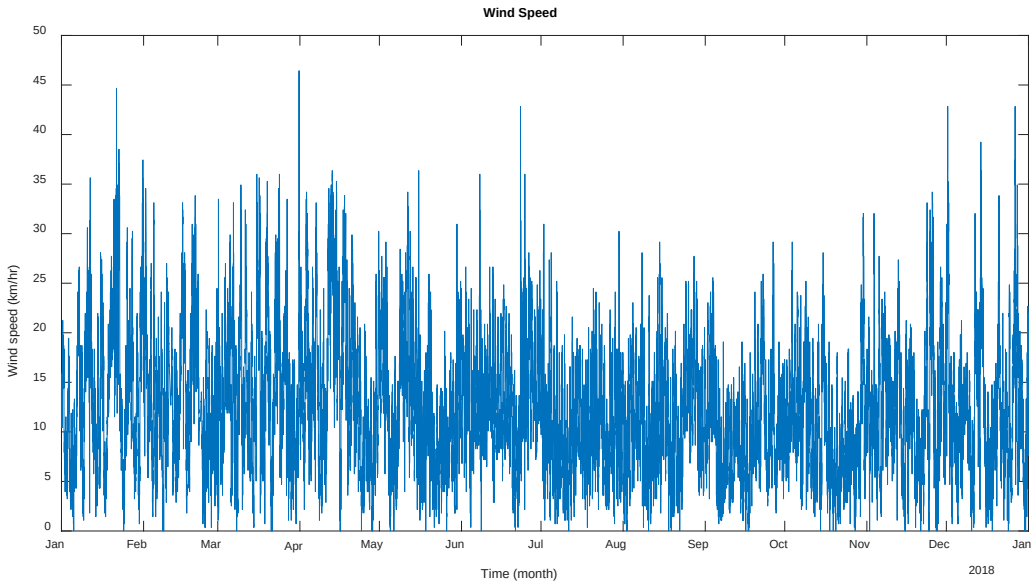

Figure 10. Climatic data collected at the ARD2 station in 2018, time series of wind speed.

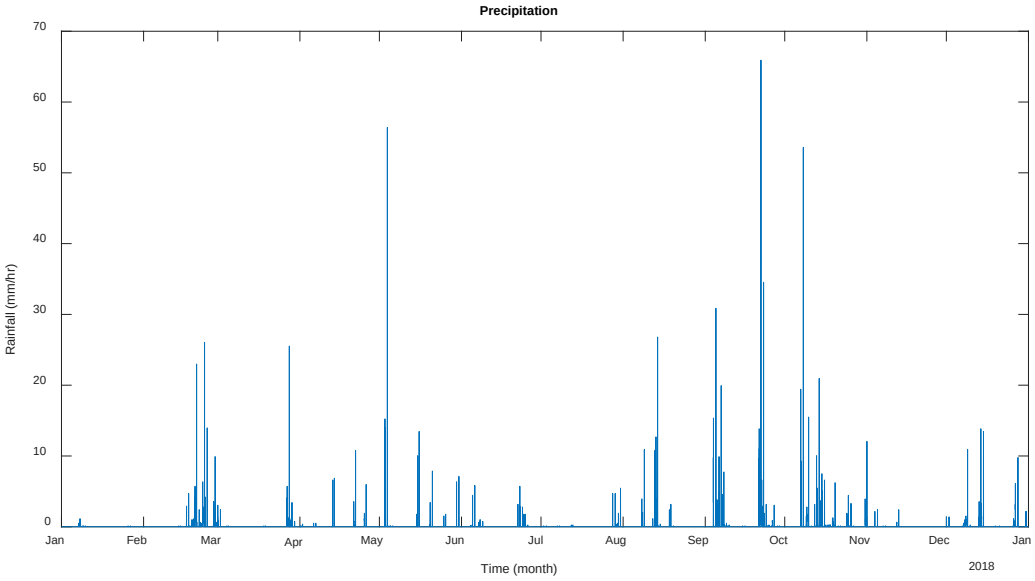

Figure 11. Climatic data collected at the ARD2 station in 2018, time series of precipitation.

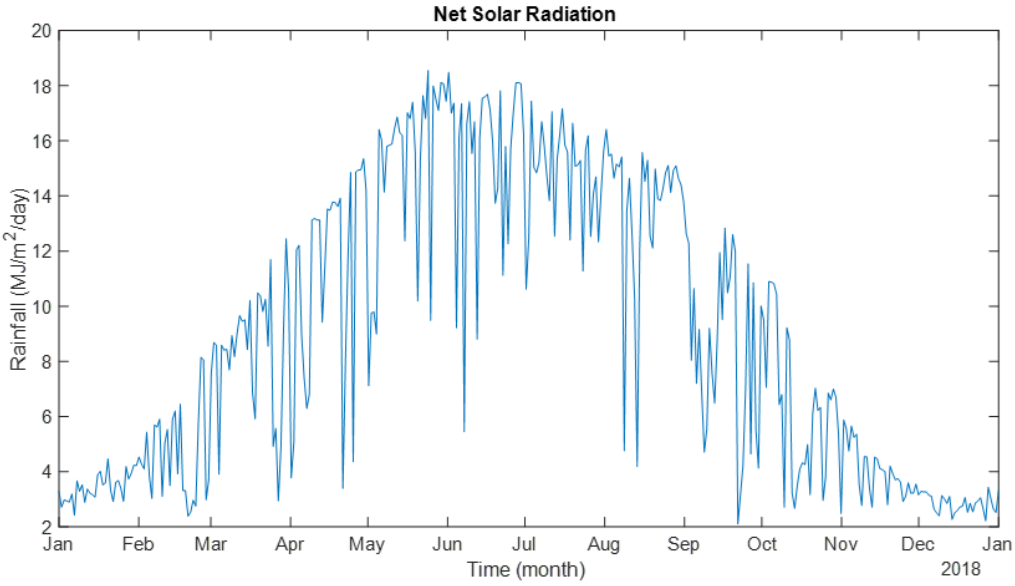

Figure 12. Climatic data collected at the ARD2 station in 2018, time series of net solar radiation.

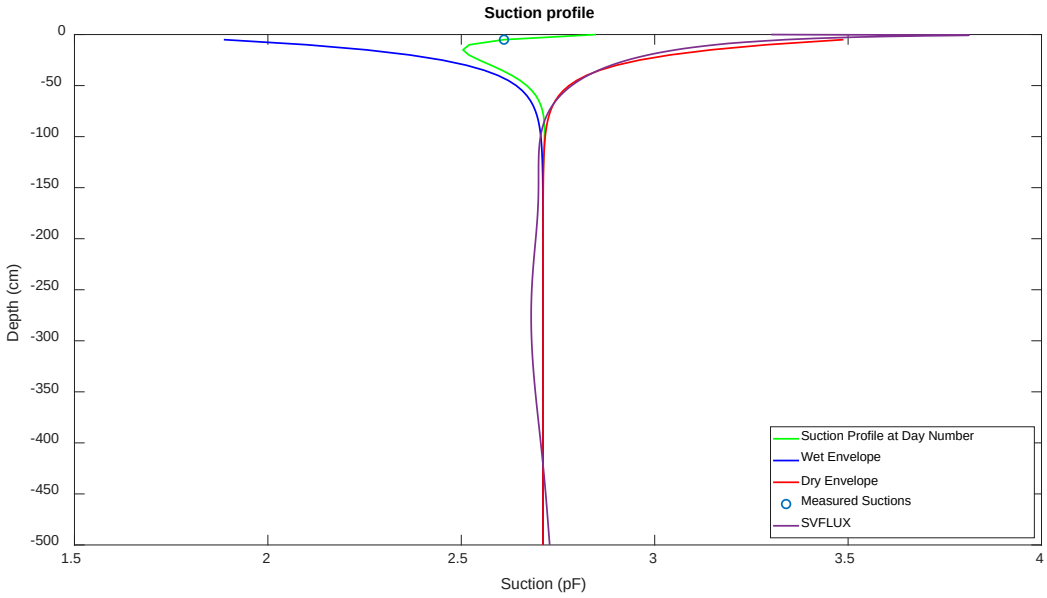

Figure 13. Predicted soil suction profiles at 09/04/2018 - ARD2 station in 2018.

5.3.2. DURA Station

The climatic data acquired from DURA station over a period of 8640 h (365 d) in 2018 are shown in Figures 14 to 18. The comparison of the results between the proposed model and FE Seepage simulation are presented in Figure 19. Overall, the proposed model and FE Seepage simulated soil suction values for DURA station over the time period of interest showed more variations near the surface. The FE Seepage simulated soil suction profile tends towards the dry boundary suction envelope while the proposed model remains in the middle of two boundaries with the predicted profile passing through the measured suction value on 09/18/2018.

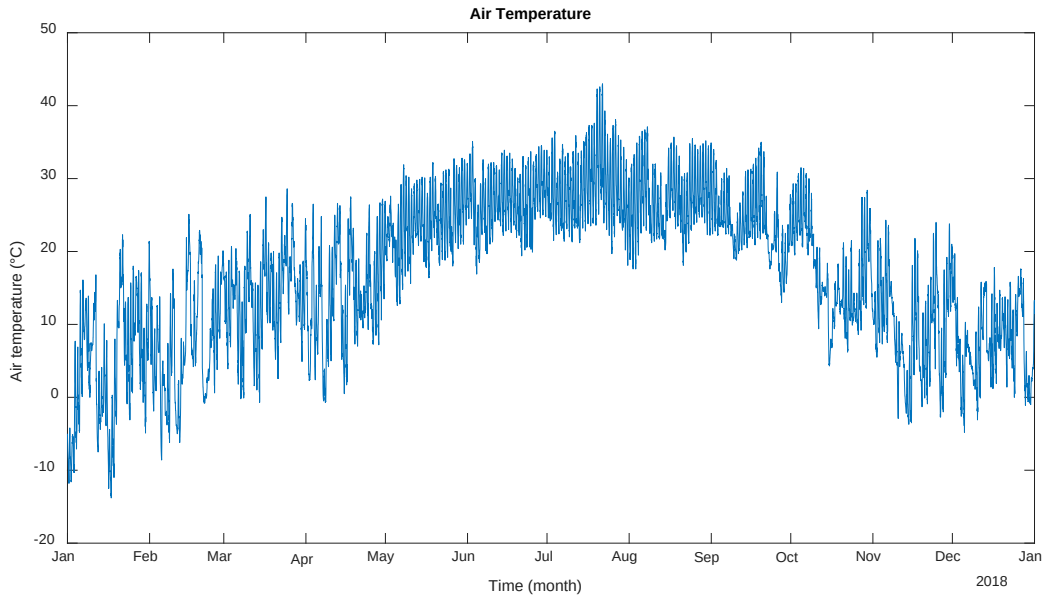

Figure 14. Climatic data collected at the DURA station in 2018, time series of air temperature.

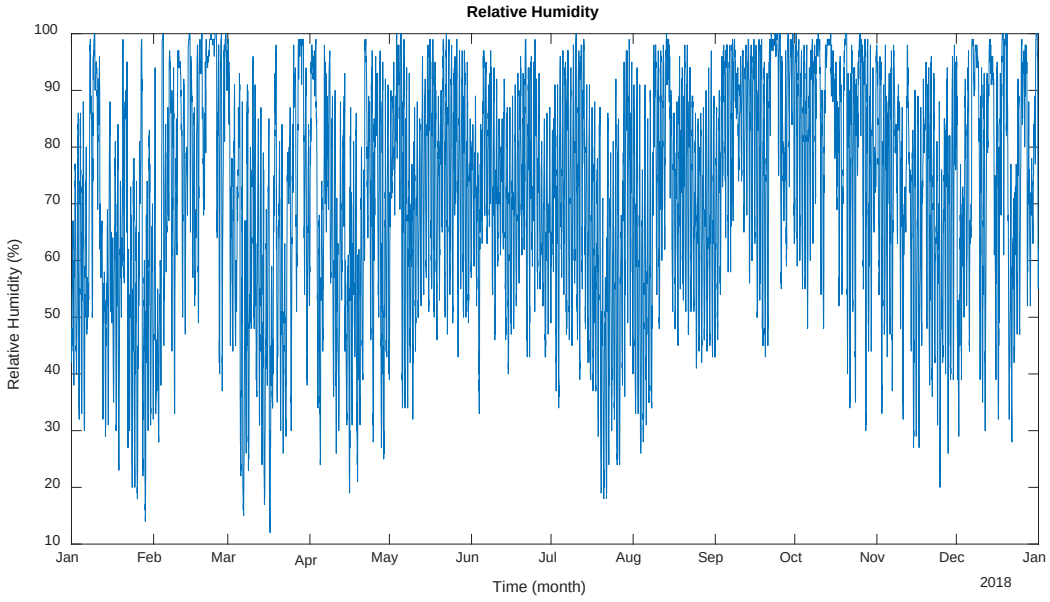

Figure 15. Climatic data collected at the DURA station in 2018, time series of relative humidity.

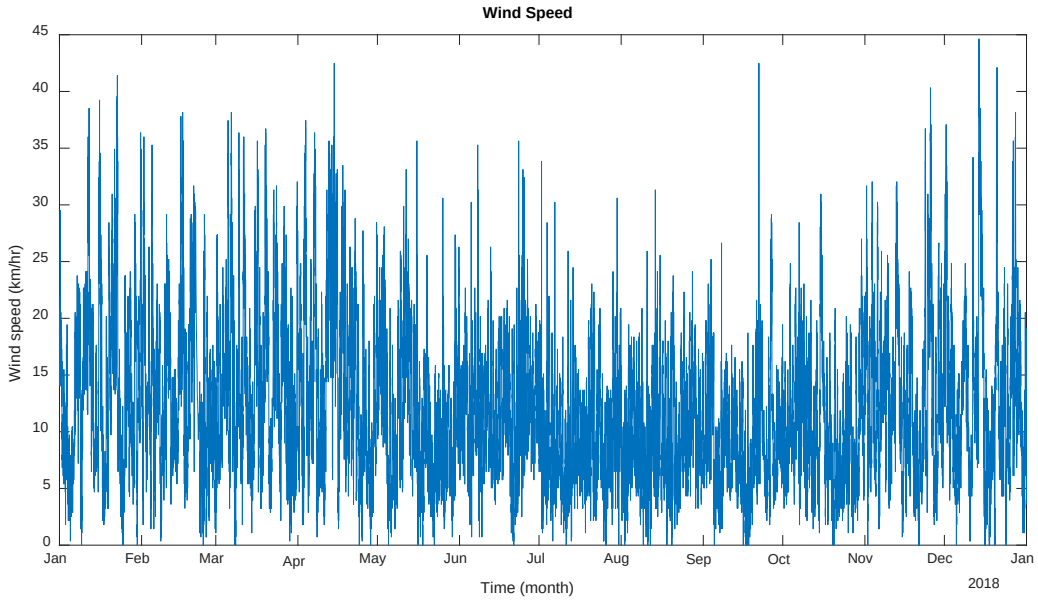

Figure 16. Climatic data collected at the DURA station in 2018, time series of wind speed.

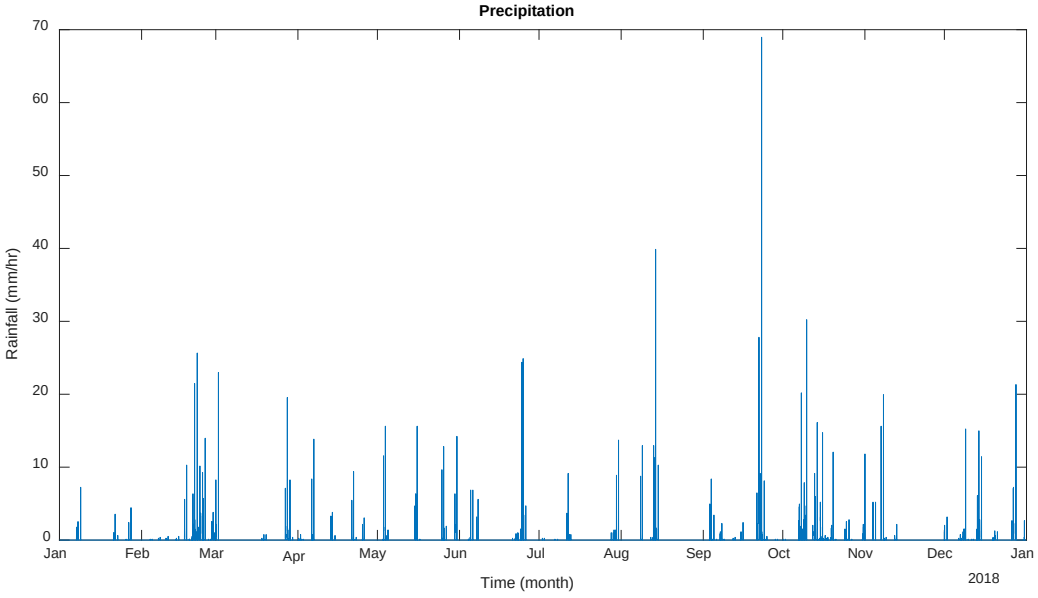

Figure 17. Climatic data collected at the DURA station in 2018, time series of precipitation.

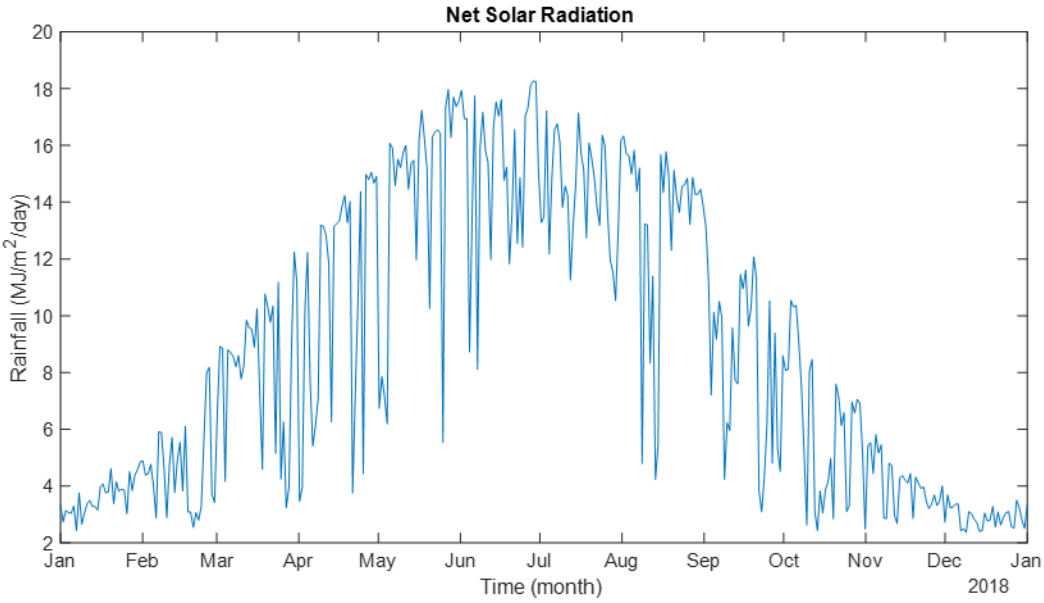

Figure 18. Climatic data collected at the DURA station in 2018, time series of net solar radiation.

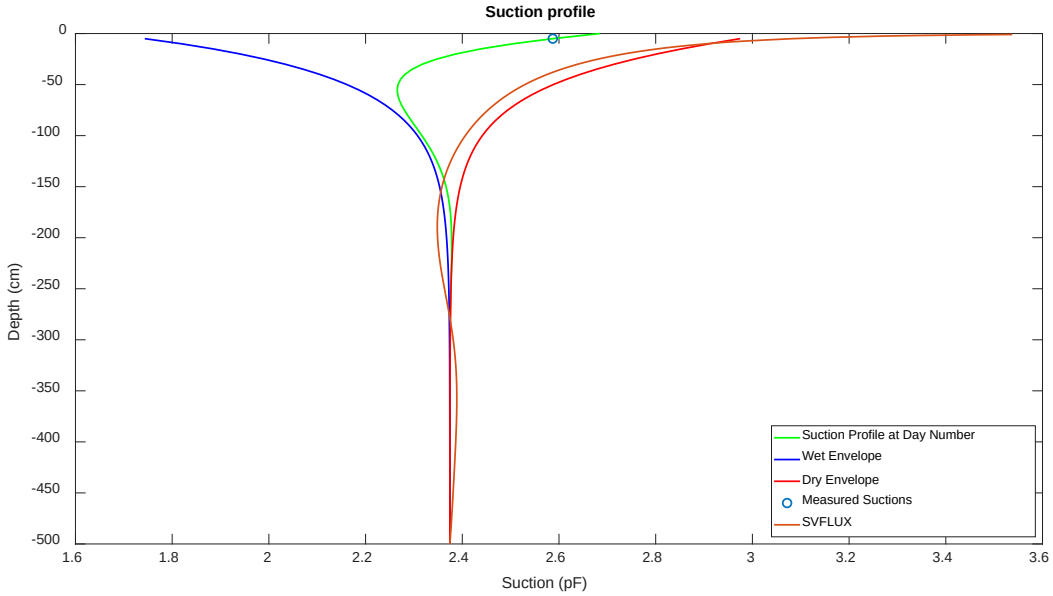

Figure 19. Predicted soil suction profile at 09/18/2018 - DURA station in 2018.

5.3.3. HUGO Station

The climatic data acquired from HUGO station over a period of 8640 h (365 d) in 2018 are shown in Figures 20 to 24. The comparison of the results between the proposed model and FE Seepage simulation are presented in Figure 25. Overall, the proposed model and FE Seepage simulated soil suction values for HUGO station for the time of the analysis (09/17/2018) showed more variations near the surface. Similar to two other stations, the FE Seepage simulated soil suction profile tends toward the dry boundary condition and predicts higher suction near the ground surface. However,

the agreement in the prediction of the profiles for 09/17/2018 from both models was slightly better for the HUGO station.

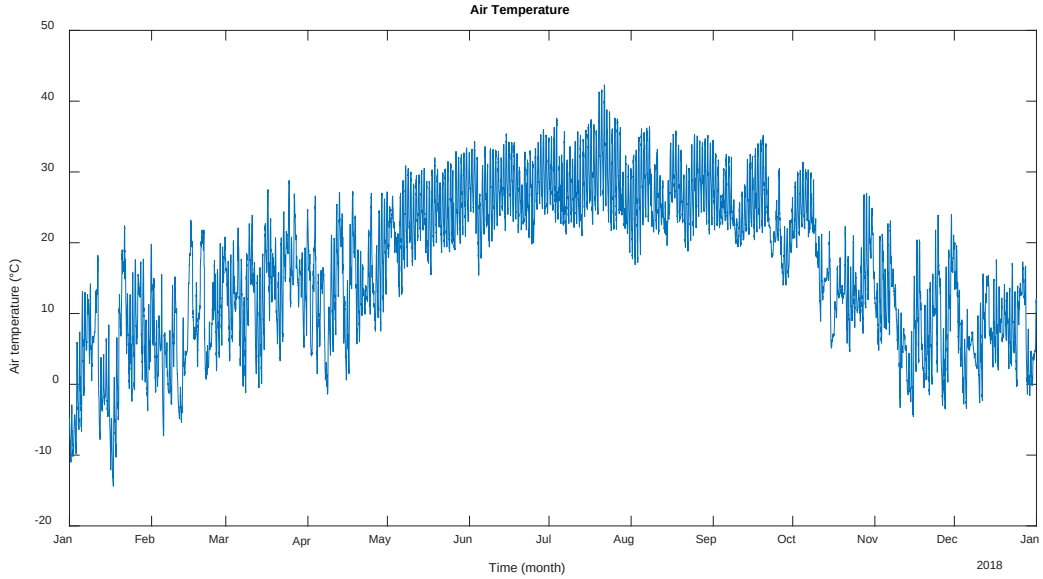

Figure 20. Climatic data collected at the HUGO station in 2018, time series of air temperature.

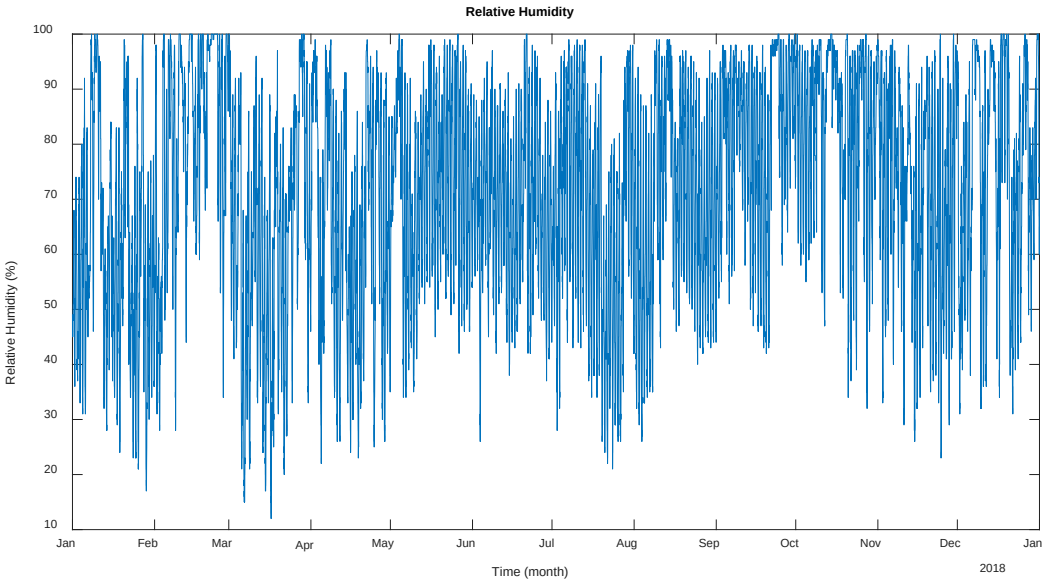

Figure 21. Climatic data collected at the HUGO station in 2018, time series of relative humidity.

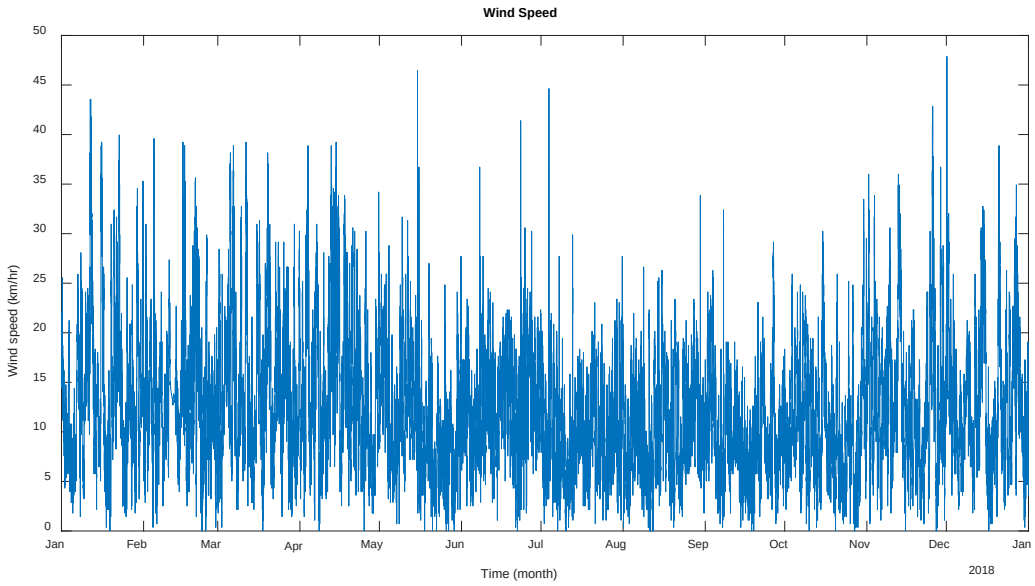

Figure 22. Climatic data collected at the HUGO station in 2018, time series of wind speed.

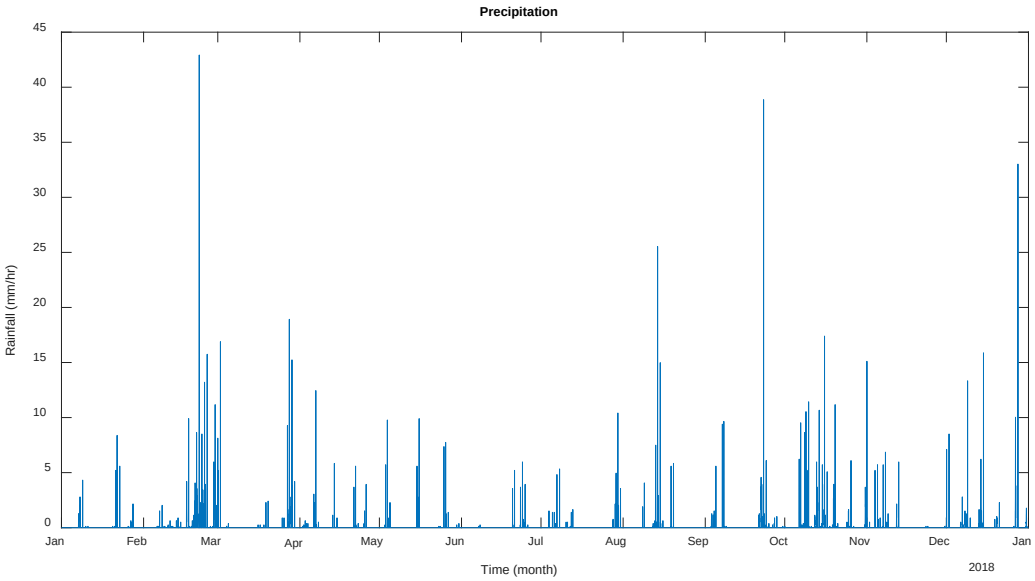

Figure 23. Climatic data collected at the HUGO station in 2018, time series of precipitation.

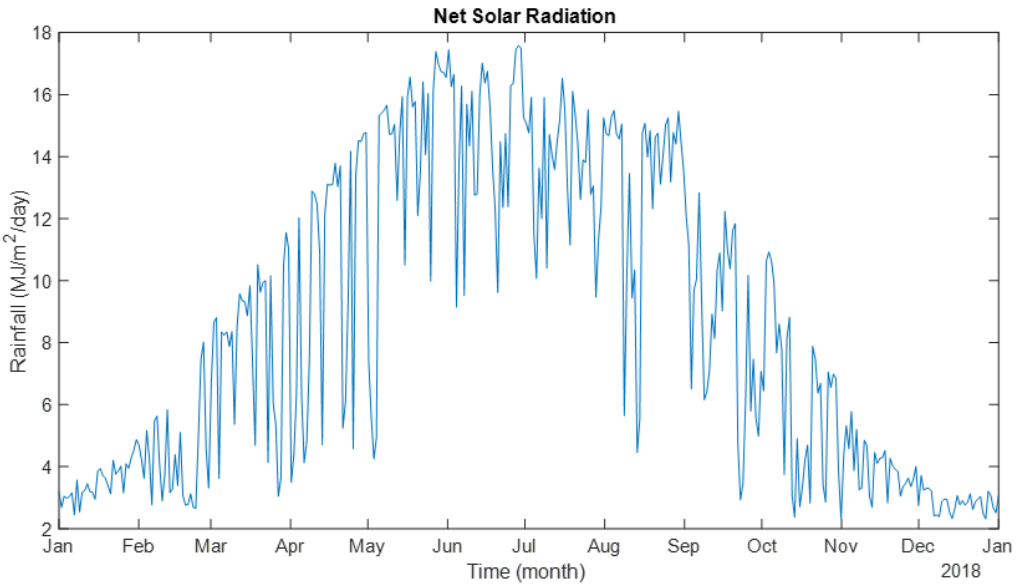

Figure 24. Climatic data collected at the HUGO station in 2018, time series of net solar radiation.

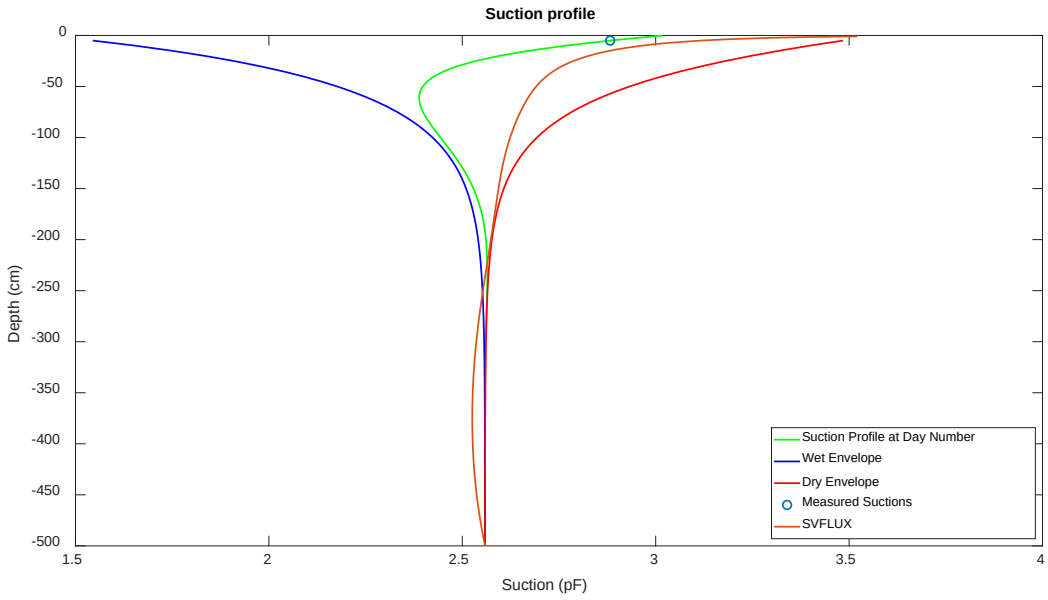

Figure 25. Predicted soil suction profile at 09/17/2018 - HUGO station in 2018.

The comparison of the results from the SVFlux and the proposed model for the three weather stations clearly indicates that the proposed model (or modified Mitchell model) suction profile predictions are in agreement with the measured suction value close to the surface at the time of the analysis. However, the SVFlux predictions are inclined more towards the dry suction envelope.

5.4. Correlation Between Environmental Parameters and Suction

Previous studies showed that the suction beneath covered areas mainly depends on climatic factors and soil properties *(28, 46, 48,55, 85-88)*. Based on the literature review, and this study, it was found out that a suitable statistical model can be developed to estimate the equilibrium suction in the subgrade soil from climatic parameters and soil properties. The environmental data were obtained from the Oklahoma Mesonet stations. The following parameters were considered in the analysis:

- Annual mean relative humidity,
- Monthly mean relative humidity,
- Annual mean temperature,
- Monthly average temperature,
- Annual precipitation,
- Annual mean sunshine,
- Annual mean windspeed,
- Annual mean percent sunshine,
- Clay content at 20cm depth,
- TMI.

The matric suction data set used in the correlations was obtained from the prediction model, as stated above.

5.4.1. Equilibrium Suction Model

In the correlation process, each data set was plotted and evaluated for significant trends. Figure 26 illustrates the correlation between the equilibrium suction and climate variables. For example, the matric suction decreased as annual mean relative humidity increased. The clay content has direct relation with suction and as clay content increases the matric suction increases.

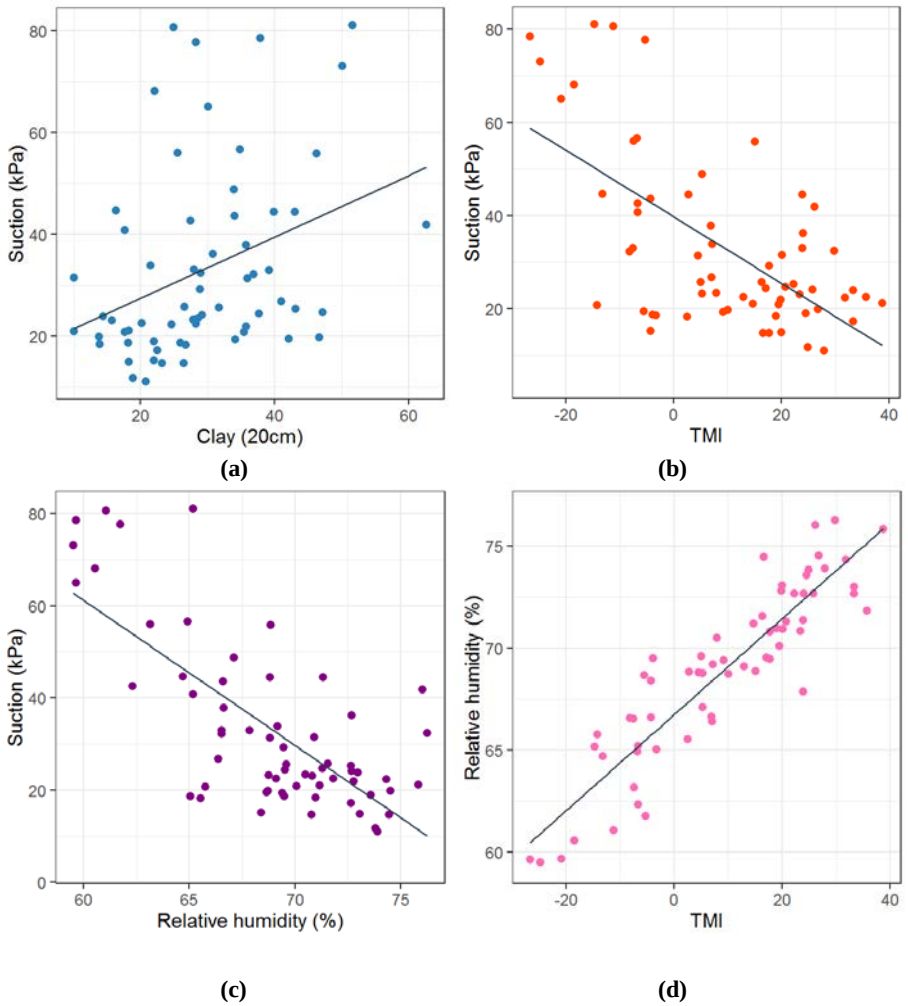

Figure 26. Correlation between the equilibrium suction and Clay content (a), TMI (b), Relative humidity (c), and Relative humidity vs. TMI (d).

The current study revealed that relative humidity (RH), clay content (%), and TMI by Thornthwaite and Mather *(65)* are statistically significant parameters and have correlation with the suction (kPa). The statistical analysis yielded suction values that decreased as TMI increased. The data set has the following range of annual mean relative humidity of 59% to 76% and clay contents of 10% to 60% at 20 cm depth.

A non-linear model was fitted to the dataset. The F-test of overall significance was used to determines whether the relationship is statistically significant for the equilibrium suction model. Results of the computation are as follows:

$$Suction = b_0 + e^{b_1 + b_2(RH) + b_3(Clay) + b_4(TMI) + b_5(RH \times TMI)} \quad [36]$$

Values of the constants obtained through the regression process are:
$b_0 = -100;$
$b_1 = 6.161;$
$b_2 = -0.0206;$
$b_3 = 0.0036;$

$b_4 = 0.0292$;
$b_5 = 0.0004$;
$R^2 = 71.4$; and
Number of observations = 70.

5.3.2. Error Analysis

To evaluate the agreement of the measured data points with the equilibrium suction model, an error analysis was performed. The suction values for each site were estimated using the new model ($S_{predicted}$) and compared with the measured values ($S_{measured}$). The absolute mean error ($e_{absolute}$) and algebraic mean error ($e_{algebraic}$) were calculated using Equations 37 and 38, where n is the number of observations.

$$e_{absolute} = \frac{\sum \left| \frac{S_{measured} - S_{predicted}}{S_{measured}} \right|}{n} \quad [37]$$

$$e_{algebraic} = \frac{\sum \left(\frac{S_{measured} - S_{predicted}}{S_{measured}} \right)}{n} \quad [38]$$

Results from the error analyses of the model were compared with the error analysis obtained from Zapata et al. *(88)* model. The analysis yielded a mean absolute error of 1.2% and mean algebraic error of 0.02%. The values for the mean absolute error and the mean algebraic error from Zapata et al. *(88)* model were found to be 9.5% and 2.1% respectively. The comparison indicates that the equilibrium suction under subgrade soil can be predicted better by utilizing relative humidity, clay content, and TMI.

5.4. Guidelines for Analyzing Relevant Climate Data for Pavement Analysis

The objective of this research study was to develop a moisture prediction model that could be used to determine the moisture distribution profile underneath the pavement structure. The moisture prediction model presented in the last two chapters can easily be programmed into spreadsheet using the guidelines presented below.

1. **Data Preparation:**
   Climate data is essential part of the proposed model in this study. Therefore, assessing the integrity of weather data used for estimating climatic variables and replacing missing data are necessary. The calculation of TMI and matric suction require measurements or estimates for air temperature, humidity, precipitation, solar radiation, and wind speed. These parameters are considered to be the minimum requirements to estimate TMI and matric suction.

   - Mean Air Temperature (T)
     For the standardized method, the mean air temperature, T, for a daily time step is preferred as the mean of the average of hourly temperature measurements to provide for consistency across all data sets.
   - Mean Relative Humidity (RH)
     For the standardized method, the mean relative humidity, RH, for a daily time step is calculated as the mean of the average of hourly relative humidity measurements to provide for consistency across all data sets.

- Daily Precipitation (R)
  For the standardized method, the daily rainfall, R, for a daily time step is calculated as the sum of the hourly rainfall measurements for a day to provide a consistency across all data sets.
- Mean Solar Radiation (SR)
  For the standardized method, the solar radiation, SR, for a daily time step is calculated as the mean of the average of hourly solar radiation measurements.
- Mean Wind Speed (W)
  For the standardized method, the wind speed, W, for a daily time step is calculated as the mean of the average of hourly wind speed measurements.

Replacing missing data in climatic variable is conducted by fitting an autoregressive model to the samples surrounding a gap. Many observed time series exhibit serial autocorrelation; that is, linear relation between lagged observations. This suggests past observations might predict current observations. The autoregressive (AR) process models the conditional mean of y_t as a function of past observations, y_{t-1}, y_{t-2}, y_{t-3}, ..., y_{t-p}.

2. Determine Daily and Monthly Matric Suction:

The hourly matric suction can be calculated indirectly through the heat dissipation capacity of the soil by measuring a temperature difference between two reference points. The Oklahoma Mesonet stations records hourly temperature difference which can be used to calculate the matric suction by using Equation 10. For the standardized method, the matric suction, *MP*, for a daily time step is calculated as the mean of the average of hourly matric suction measurements. Similarly mean monthly matric suction can be calculated from daily matric suction.

3. Determine Fourier coefficients:

The *m* Fourier Coefficients for 12-month period can be determined from Equation 32 by using the 12 months average surface suctions.

$$U_m = \frac{2}{12}\left[\int_0^1 S_1 \cos\frac{m\pi t}{6}\,dt + \int_1^2 S_2 \cos\frac{m\pi t}{6}\,dt + \cdots + \int_{11}^{12} S_{12} \cos\frac{m\pi t}{6}\,dt\right] \quad [32]$$

where:

$S_1, S_2, \ldots, S_{12}$ = Monthly average of the surface suction; and

$m = 0, 1, 2, \ldots$

4. Determine the diffusion coefficient:

Diffusion coefficient for any day can be back calculated by solving Equation 30 for the measured suction for the target day. The solving procedure is as follows:

a) Assume an initial value for diffusion coefficient such as 0.01 cm^2/s.
b) Calculate the matric suction at the measured suction depth (i.e., 5 cm or 25 cm) by using the Fourier coefficient from previous step and Equation 30.
c) Calculate the difference between predicted the matric suction and measured suction from a weather station.

d) If the difference between predicted and measured matric suction are less than 0.001 pF then the diffusion coefficient is found else repeat the process until a reasonable tolerance amount is reached.

5. Determine suction distribution with depth in the subgrade:

The suction distribution profile for the selected day number can be estimated by using the diffusion coefficient obtained from the previous step and calculating the suction at any depth y using Equation 30.

$$u(y,t) = \frac{U_o}{2} + U_1 \, e^{-y\sqrt{((n\pi/\alpha))}} \cos(n2\pi t - y\sqrt{(n\pi/\alpha)}) + U_2 \, e^{-y\sqrt{(2n\pi/\alpha)}} \cos(2n2\pi t - y\sqrt{(2n\pi/\alpha)}) + \cdots etc. \quad [30]$$

where:

y = Depth of measured suction;

$t = \frac{Day\ number}{2\times365}$; and

$U_0, U_1, U_2 \ldots . etc..$ = Fourier Coefficients which can determined from Equation 32.

6. Construct the suction distribution profile:

The final step is to construct the suction distribution profile by plotting the estimated matric suction against the depth.

6. CONCLUSIONS

This study mainly focused on improving our understanding of environmental interactions with pavement systems for better predictions of the changes in pavement material properties over time. The main objective of this study was to develop a practical and implementable numerical model for predicting the moisture regime within the pavement subgrade system. The research study resulted in a rational and practical prediction model that could be used to determine the moisture boundary conditions within the pavement structure. The proposed moisture variation model was tested, and the results were compared with the predicted values from a well-established climatic model in the SVFlux software. The proposed model successfully used the measured suction from the field and predicted a more realistic suction profile as compared to the prediction made by the SVFlux. Furthermore, the proposed model is able to compute the diffusion coefficient based on the predicted suction profile.

The moisture prediction model presented in this study can be used to predict equilibrium moisture beneath the pavement as well. The numerical modelling was utilized to predict the equilibrium matric suction from measurements of suction data in the field. The modified Mitchell model was also successfully utilized the measured suction from the field for computing the diffusion coefficient. The diffusion coefficient is extremely important in estimating moisture penetration into soil profile. The model can easily be programmed into a spreadsheet using the equations presented in this study.

On the basis of the field data and numerical modeling, a statistical based model was also developed to build a relationship between equilibrium suction of subgrade soils, TMI, relative humidity and clay content. The matric suction under the unbound layer beneath the pavement can be estimated with environmental parameters and clay content. TMI and relative humidity are found to be controlling parameters in predicting equilibrium matric suction. The TMI, which effectively quantifies the environmental factors for a given region, can be obtained from contour maps developed in this study.

Thornthwaite Moisture Index (TMI) controls the moisture boundary conditions in the pavement profile. In this study, large cluster of raw climate and soil moisture data were obtained from Oklahoma Mesonet for assessment of the TMI from 1994 to 2017. Extensive computations have been carried out and TMI values were calculated for 77 Mesonet weather stations representing 77 counties in the state. Thornthwaite Moisture Index (TMI) contour maps were created for Oklahoma using two different models (i.e., Thornthwaite and Mather *(65)* and Witczak et al. *(57)*).

The results of this study have led to important recommendations that could be considered in improving the climatic data and moisture (suction) boundary conditions for the mechanistic empirical design guide. Using the current and historical climatic data pertaining to Oklahoma future trends of the climatic parameters could be predicted using proposed models. It must also be noted that the data and procedure developed are based upon Mesonet weather data at specific sites in Oklahoma, subjected to specific weather and drainage conditions. It is expected that alterations in drainage (i.e., ponding) or in the soil fabric (i.e., deeper cracks) would result in different predictions. Additional field observations and studies are needed to expand the database to other climates, drainage conditions, and soil fabrics.

REFERENCES

1. Puppala, A. J., T. Manosuthikij, L. Hoyos, and S. Nazarian. Moisture and Suction in Clay Subgrades Prior to Initiation of Pavement Cracking.In, 2009.

2. Nazarian, S., M. Mazari, I. Abdallah, A. Puppala, L. Mohammad, and M. Abu-Farsakh. *Modulus-based construction specification for compaction of earthwork and unbound aggregate*. Transportation Research Board, 2015.

3. Dempsey, B., W. Herlach, and A. Patel. The Climatic-Material-Structural Pavement Analysis Program, Vol. 3, Final Report.In, FHWARD-84/115. FHWA, US Department of Transportation, Washington DC, 1985.

4. Guymon, G. L., R. L. Berg, and T. V. Hromadka. Mathematical model of frost heave and thaw settlement in pavements.In, Cold Regions Research And Engineering Lab Hanover NH, 1993.

5. Liu, S., and R. Lytton. Environmental effects on pavement-drainage. *Volume IV, Federal Highway Administration, Report FHWA-DTFH-61-87-C-00057*, 1985.

6. Shang, H. Rainfall estimation for pavement analysis and design. *Design, Management, and Operation of Pavements*, 1988, p. 42.

7. Lytton, R., D. Pufahl, C. Michalak, H. Liang, and B. Dempsey. An integrated model of the climatic effects on pavements. 1993.

8. Larson, G., and B. J. Dempsey. Enhanced integrated climatic model Version 2.0.In, Department of Civil and Environmental Engineering, 1997.

9. Gupta, S., A. Ranaivoson, T. Edil, C. Benson, and A. Sawangsuriya. Pavement design using unsaturated soil technology. 2007.

10. McCartney, J. S., and A. Khosravi. Field-monitoring system for suction and temperature profiles under pavements. *Journal of Performance of Constructed Facilities*, Vol. 27, No. 6, 2012, pp. 818-825.

11. Bayomy, F., and H. Salem. Monitoring and Modeling Subgrade Soil Moisture for Pavement Design and Rehabilitation in Idaho.In, Phase III: Data Collection and Analysis, Final Report, revised and re-submitted May, 2005.

12. Birgisson, B., J. Ovik, and D. Newcomb. Analytical predictions of seasonal variations in flexible pavements: Minnesota road research project site. *Transportation Research Record: Journal of the Transportation Research Board*, No. 1730, 2000, pp. 81-90.

13. Ahmed, Z., I. Marukic, S. Zaghloul, and N. Vitillo. Validation of enhanced integrated climatic model predictions with New Jersey seasonal monitoring data. *Transportation Research Record: Journal of the Transportation Research Board*, No. 1913, 2005, pp. 148-161.

14. Zaghloul, S., A. Ayed, A. El Halim, N. Vitillo, and R. Sauber. Investigations of environmental and traffic impacts on mechanistic-empirical pavement design guide predictions. *Transportation Research Record: Journal of the Transportation Research Board*, No. 1967, 2006, pp. 148-159.

15. Liang, R., K. Al-Akhras, and S. Rabab'ah. Field monitoring of moisture variations under flexible pavement. *Transportation Research Record: Journal of the Transportation Research Board*, No. 1967, 2006, pp. 160-172.

16. Zapata, C. E., and W. N. Houston. *Calibration and validation of the enhanced integrated climatic model for pavement design*. Transportation Research Board, 2008.

17. Marr, S. A., R. B. Gilbert, and A. F. Rauch. A practical method for predicting expansive soil behavior.In, 2004.

18. Briaud, J.-L., X. Zhang, and S. Moon. Shrink test–water content method for shrink and swell predictions. *Journal of Geotechnical and Geoenvironmental Engineering*, Vol. 129, No. 7, 2003, pp. 590-600.

19. Overton, D. D., K.-C. Chao, and J. D. Nelson. Time rate of heave prediction for expansive soils.In *GeoCongress 2006: Geotechnical Engineering in the Information Technology Age*, 2006. pp. 1-6.

20. Richards, B. Measurement of free energy of soil moisture by the psychrometric technique, using thermistors.In, 1965.

21. Lytton, R. L., and R. K. Kher. *Prediction of moisture movement in expansive clays*. Center for Highway Research, University of Texas at Austin, 1970.

22. Mitchell, P. W. The structural analysis of footings on expansive soil.In *Expansive Soils*, ASCE, 1980. pp. 438-447.

23. Pufahl, D., and R. Lytton. Temperature and suction profiles beneath highway pavements: computed and measured. *Transportation Research Record*, Vol. 1307, 1991, pp. 268-276.

24. Fredlund, D. An introduction to unsaturated soil mechanics.In *Unsaturated Soil Engineering Practice*, ASCE, 1997. pp. 1-37.

25. Wray, W. Mass transfer in unsaturated soils: A review of theory and practices.In *Proceedings of the Second International Conference on Unsaturated Soils Volume 2*, 1998.

26. Fredlund, D., and V. Hung. Prediction of volume change in an expansive soil as a result of vegetation and environmental changes.In *Expansive Clay Soils and Vegetative Influence on Shallow Foundations*, 2001. pp. 24-43.

27. Richards, B. Behaviour of unsaturated soils. 1974.

28. McKeen, R. G., and L. D. Johnson. Climate-controlled soil design parameters for mat foundations. *Journal of Geotechnical Engineering*, Vol. 116, No. 7, 1990, pp. 1073-1094.

29. Bratton, W. Parameters for predicting shrink/heave beneath slab-on-ground foundations over expansive clays.In, PhD dissertation, Texas Tech Univ., Lubbock, Tex, 1991.

30. Lytton, R. L. Prediction of movement in expansive clays.In *Vertical and horizontal deformations of foundations and embankments*, ASCE, 1994. pp. 1827-1845.

31. Wray, W., B. El-Garhy, and A. Youssef. Three-dimensional model for moisture and volume changes prediction in expansive soils. *Journal of Geotechnical and Geoenvironmental Engineering*, Vol. 131, No. 3, 2005, pp. 311-324.

32. Adem, H., and S. Vanapalli. Constitutive modeling approach for estimating 1-D heave with respect to time for expansive soils. *International Journal of Geotechnical Engineering*, Vol. 7, No. 2, 2013, pp. 199-204.

33. Horton, R. E. The role of infiltration in the hydrologic cycle. *Eos, Transactions American Geophysical Union*, Vol. 14, No. 1, 1933, pp. 446-460.

34. Kostiakov, A. N. On the dynamics of the coefficient of water percolation in soils and the necessity of studying it from the dynamic point of view for the purposes of amelioration. *Trans. Sixth Comm. Int. Soc. Soil Sci.*, Vol. 1, 1932, pp. 7-21.

35. Freeze, R. A., and J. A. Cherry. Groundwater Prentice-Hall Inc. *Eaglewood Cliffs, NJ*, 1979.

36. Gitirana Jr, G. Weather-related geo-hazard assessment model for railway embankment stability.In, 2005.

37. Vu, H. Q., and D. G. Fredlund. The prediction of one-, two-, and three-dimensional heave in expansive soils. *Canadian Geotechnical Journal*, Vol. 41, No. 4, 2004, pp. 713-737.

38. Gitirana Jr, G., and D. G. Fredlund. Infiltration-runoff boundary conditions in seepage analysis. *sat*, Vol. 1, 2005, p. 3.

39. Gardner, W. Some steady-state solutions of the unsaturated moisture flow equation with application to evaporation from a water table. *Soil Science*, Vol. 85, No. 4, 1958, pp. 228-232.

40. Van Genuchten, M. T. A closed-form equation for predicting the hydraulic conductivity of unsaturated soils 1. *Soil Science Society of America Journal*, Vol. 44, No. 5, 1980, pp. 892-898.

41. Fredlund, D. G., and A. Xing. Equations for the soil-water characteristic curve. *Canadian Geotechnical Journal*, Vol. 31, No. 4, 1994, pp. 521-532.

42. Fredlund, D., A. Xing, and S. Huang. Predicting the permeability function for unsaturated soils using the soil-water characteristic curve. *Canadian Geotechnical Journal*, Vol. 31, No. 4, 1994, pp. 533-546.

43. Leong, E. C., and H. Rahardjo. Permeability functions for unsaturated soils. *Journal of Geotechnical and Geoenvironmental Engineering,* Vol. 123, No. 12, 1997, pp. 1118-1126.

44. Abed, A. A. Numerical modeling of expansive soil behavior.In, IGS, 2008.

45. Brinkgreve, R., R. Al-Khoury, and J. Van Esch. Plaxflow User Manual Version 1.4.In, Balkema, The Netherlands, 2006.

46. Aitchison, G. Moisture equilibria and moisture changes in soils beneath covered areas. 1965.

47. Basma, A. A., and T. I. Al-Suleiman. Climatic considerations in new AASHTO flexible pavement design. *Journal of Transportation Engineering,* Vol. 117, No. 2, 1991, pp. 210-223.

48. Russam, K., and J. Coleman. The effect of climatic factors on subgrade moisture conditions. *Géotechnique,* Vol. 11, No. 1, 1961, pp. 22-28.

49. Coleman, J. Geology, climate and vegetation as factors affecting soil moisture. *Moisture Equilibria and Moisture Changes in Soils Beneath Covered Areas. Butterworth, Sydney, Australia*, 1965, pp. 93-99.

50. Thornthwaite, C. W. An approach toward a rational classification of climate. *Geographical review*, Vol. 38, No. 1, 1948, pp. 55-94.

51. Carpenter, S. H., R. L. Lytton, and J. A. Epps. Environmental Factors Relevant to Pavement Cracking in West Texas.In, Texas Transportation Institute, Texas A & M University, 1974.

52. Edris, E. V., and R. L. Lytton. Dynamic properties of subgrade soils, including environmental effects.In, Texas A&M University., 1976.

53. Lytton, R., C. Aubeny, and R. Bulut. Design Procedure for Pavements on Expansive Soils.In, Texas Transportation Institute, 2005.

54. Gay, D. A. Development of a predictive model for pavement roughness on expansive clay. 1995.

55. Fredlund, D. G., and H. Rahardjo. *Soil mechanics for unsaturated soils*. John Wiley & Sons, 1993.

56. Zapata, C. E. Uncertainty in soil-water-characteristic curve and impacts on unsaturated shear strength predictions. 2000.

57. Witczak, M., C. Zapata, and W. Houston. Models incorporated into the current enhanced integrated climatic model: NCHRP 9-23 project findings and additional changes after version 0.7. *Final Report, Project NCHRP,* 2006.

58. Saha, S., N. Hariharan, F. Gu, X. Luo, D. N. Little, and R. L. Lytton. Development of a Mechanistic-Empirical Model to Predict Equilibrium Suction for Subgrade Soil. *Journal of Hydrology,* 2019.

59. Illston, B. G., J. B. Basara, C. A. Fiebrich, K. C. Crawford, E. Hunt, D. K. Fisher, R. Elliott, and K. Humes. Mesoscale monitoring of soil moisture across a statewide network. *Journal of Atmospheric and Oceanic Technology*, Vol. 25, No. 2, 2008, pp. 167-182.

60. Bulut, R., and E. C. Leong. Indirect measurement of suction.In *Laboratory and Field Testing of Unsaturated Soils*, Springer, 2008. pp. 21-32.

61. Illston, B. G., J. B. Basara, and K. C. Crawford. Seasonal to interannual variations of soil moisture measured in Oklahoma. *International Journal of Climatology: A Journal of the Royal Meteorological Society*, Vol. 24, No. 15, 2004, pp. 1883-1896.

62. National Cooperative Highway Research Program (NCHRP). "Guide for mechanistic-empirical design of new and rehabilitated pavement structures." *National Cooperative Highway Research Program 1-37 A* (2004).

63. Heitzman, M., D. Timm, E. S. Tackle, D. E. Herzmann, and D. D. Traux. Developing MEPDG Climate Data Input Files for Mississippi.In, 2011.

64. Allen, R., I. Walter, R. Elliott, R. Howell, D. Itenfisu, and M. Jensen. RL Snyder, The ASCE Standardized Reference Evapotranspiration Equation.In, Environmental and Water Resources Institute of the American Society of Civil …, 2005.

65. Thornthwaite, C., and R. Mather. The water balance publication in climatology, 8 (1) DIT. *Laboratory of Climatology, Centerton, NJ 104p*, 1955.

66. Thode, R., and G. Gitiriana. SvFlux theory manual. *Soilvision Systems Ltd., Sakatchewan, Canada*, 2008.

67. Bear, J. *Dynamics of fluids in porous media*. Courier Corporation, 2013.

68. Philip, J., and D. De Vries. Moisture movement in porous materials under temperature gradients. *Eos, Transactions American Geophysical Union*, Vol. 38, No. 2, 1957, pp. 222-232.

69. Dakshanamurthy, V., and D. Fredlund. A mathematical model for predicting moisture flow in an unsaturated soil under hydraulic and temperature gradients. *Water Resources Research*, Vol. 17, No. 3, 1981, pp. 714-722.

70. Zapata, C. E., W. N. Houston, S. L. Houston, and K. D. Walsh. Soil–water characteristic curve variability.In *Advances in Unsaturated Geotechnics*, 2000. pp. 84-124.

71. Mualem, Y. A new model for predicting the hydraulic conductivity of unsaturated porous media. *Water Resources Research*, Vol. 12, No. 3, 1976, pp. 513-522.

72. Vereecken, H., J. Maes, J. Feyen, and P. Darius. Estimating the soil moisture retention characteristic from texture, bulk density, and carbon content. *Soil Science*, Vol. 148, No. 6, 1989, pp. 389-403.

73. Brooks, R. H., and A. T. Corey. Hydraulic properties of porous media and their relation to drainage design. *Transactions of the ASAE,* Vol. 7, No. 1, 1964, pp. 26-0028.

74. Campbell, G. S. A simple method for determining unsaturated conductivity from moisture retention data. *Soil Science,* Vol. 117, No. 6, 1974, pp. 311-314.

75. Burdine, N. Relative permeability calculations from pore size distribution data. *Journal of Petroleum Technology,* Vol. 5, No. 3, 1953, pp. 71-78.

76. Wilson, G. W. Soil evaporative fluxes for geotechnical engineering problems. 1990.

77. Penman, H. L. Natural evaporation from open water, bare soil and grass. *Proceedings of the Royal Society of London. Series A. Mathematical and Physical Sciences,* Vol. 193, No. 1032, 1948, pp. 120-145.

78. Gray, D. M. *Handbook on the Principles of Hydrology: with special emphasis directed to Canadian conditions in the discussions, applications and presentation of data*. Secretariat, Canadian National Committee for the International Hydrological …, 1970.

79. Wetzel, P. J., and A. Boone. A Parameterization for Land–Atmosphere-Cloud Exchange (PLACE): Documentation and testing of a detailed process model of the partly cloudy boundary layer over heterogeneous land. *Journal of Climate,* Vol. 8, No. 7, 1995, pp. 1810-1837.

80. Lowe, P. R. An approximating polynomial for the computation of saturation vapor pressure. *Journal of Applied Meteorology,* Vol. 16, No. 1, 1977, pp. 100-103.

81. Walter, I. A., R. G. Allen, R. Elliott, M. Jensen, D. Itenfisu, B. Mecham, T. Howell, R. Snyder, P. Brown, and S. Echings. ASCE's standardized reference evapotranspiration equation.In *Watershed management and operations management 2000,* 2000. pp. 1-11.

82. Vision, S. SVFlux, Saturated. *Unsaturated Finite Element 2D/3D Seepage Modeling*, 2009.

83. Scott, B. L., T. E. Ochsner, B. G. Illston, C. A. Fiebrich, J. B. Basara, and A. J. Sutherland. New soil property database improves Oklahoma Mesonet soil moisture estimates. *Journal of Atmospheric and Oceanic Technology,* Vol. 30, No. 11, 2013, pp. 2585-2595.

84. Fredlund, M., J. Zhang, D. Tran, and D. Fredlund. Coupling heat and moisture flow for the computation of actual evaporation.In *Proceedings of the Canadian Geotechnical Conference and Fifth Pan-American Conference, Toronto, Ont,* 2011. pp. 2-6.

85. Bulut, R., E. Yue, L. Chen, K. Muraleetharan, M. Zaman, H. Soltani, and Z. Hossain. Evaluation of the enhanced integrated climatic model for specification of subgrade soils in Oklahoma.In, Research Report No. FHWA-OK-14-15, Oklahoma Department of Transportation, 2014.

86. De Bruijn, C. M. A. *Some observations on soil moisture conditions beneath and adjacent to tarred roads and other surface treatments in South Africa*. Butterworth & Company (Australia) Limited, 1965.

87. Smettem, K., and P. Gregory. The relation between soil water retention and particle size distribution parameters for some predominantly sandy Western Australian soils. *Soil Research,* Vol. 34, No. 5, 1996, pp. 695-708.

88. Zapata, C., Y. Perera, and W. Houston. Matric suction prediction model in new AASHTO mechanistic-empirical pavement design guide. *Transportation Research Record: Journal of the Transportation Research Board,* No. 2101, 2009, pp. 53-62.